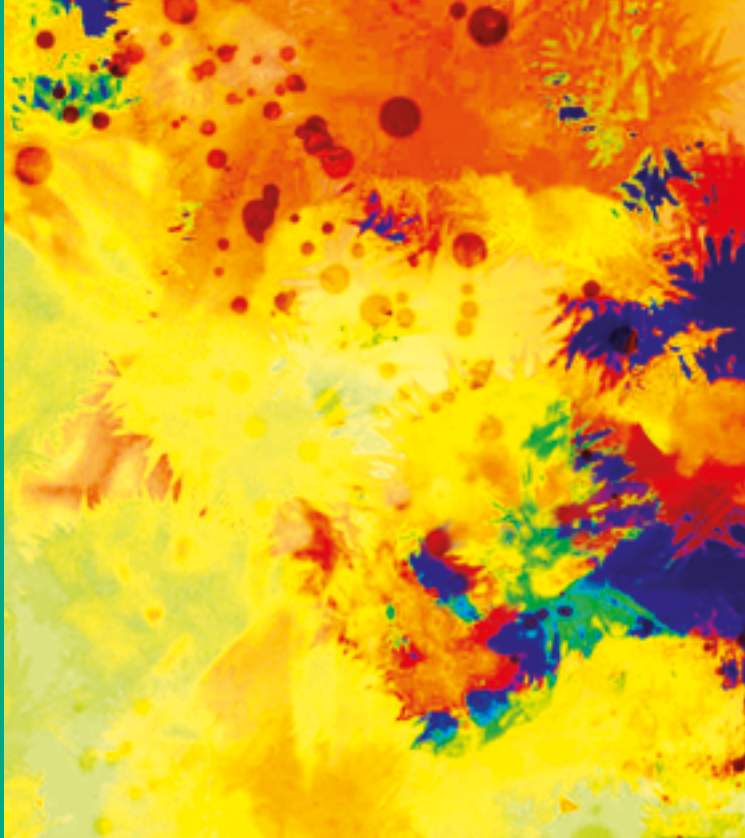


Jana Brunová
Josef Bruna



CLINICAL ENDOCRINOLOGY AND DIAGNOSTIC IMAGING

CLINICAL ENDOCRINOLOGY AND DIAGNOSTIC IMAGING

MUDr. Jana Brunová, CSc. Prof.h.c.
Prof. MUDr. Josef Bruna, DrSc., Dr.h.c.

Reviewed by:
Prof. MUDr. Karel Benda, DrSc.
Prof. MUDr. Petr Vlček, CSc.

Published by Charles University in Prague, Karolinum Press
Prague 2014
Edited by Jana Jindrová
Proofread by Peter Kirk Jensen
Layout and typeset by Kateřina Řezáčová
First edition

© Charles University in Prague, 2014
© Jana Brunová, Josef Bruna, 2014

ISBN 978-80-246-2058-9
ISBN 978-80-246-2079-6 (online : pdf)



Univerzita Karlova v Praze
Nakladatelství Karolinum 2014

<http://www.cupress.cuni.cz>

Authors

MUDr. Jana Brunová, CSc., Prof.h.c.

- Head of Endocrine Clinic, Diabetes Centre of Institute for Clinical and Experimental Medicine, Lecturer of the 3rd Faculty of Medicine, Charles University in Prague, Czech Republic
- Professor Honoris Causa of Faculty of Medicine, University of Valença, Rio de Janeiro, Brazil
- Former Consultant of Endocrine Clinic and Department of Internal Medicine, Faculty of Health Sciences and University Hospitals, University of the Free State, Bloemfontein, Republic of South Africa

Prof. MUDr. Josef Bruna, DrSc., Dr.h.c.

- Professor of Radiology, the 2nd Faculty of Medicine, Charles University in Prague, University Hospital in Motol, Czech Republic
- Doctor Honoris Causa of Faculty of Medicine, University of Valença, Rio de Janeiro, Brazil
- Former Senior Consultant and Temporary Head of the Department of Diagnostic Radiology, Faculty of Health Sciences and University Hospitals, University of the Free State, Bloemfontein, Republic of South Africa

Contents

Preface	11
Introduction	13
1. PITUITARY GLAND	15
1.1 Embryology remarks	15
1.2 Anatomy remarks	16
1.3. Imaging of the pituitary region	20
1.4 Pituitary adenomas	26
1.4.1 Hyperprolactinemia and prolactinoma	33
1.4.2 Acromegaly and somatotrophic adenoma	38
1.4.3 Adrenocorticotrophic adenoma	44
1.4.4 Gonadotroph cell adenoma	44
1.4.5 Thyrotroph cell adenoma	44
1.4.6 Plurihormonal pituitary adenoma	46
1.4.7 Pituitary incidentaloma	47
1.4.8 Nonfunctioning adenoma	50
1.5 Hypopituitarism.	50
1.5.1 Symptoms of pituitary space-occupying lesion	51
1.5.2 Symptoms of hormonal deficiency.	53
1.6 Other sellar and parasellar pathology.	63
1.6.1 Pituitary gland hyperplasia	63
1.6.2 Pituitary cysts	63
1.6.3 Craniopharyngioma.	63
1.6.4 Meningioma	63
1.6.5 Empty sella	64
1.6.6 Transsphenoidal encephalocele	64
1.6.7 Septo-optic dysplasia	65
1.6.8 Hypoplasia of the pituitary gland	65
1.6.9 Inflammation and infection	65
1.6.10 Lymphocytic autoimmune hypophysitis.	66
1.6.11 Hemochromatosis	66
1.6.12 Hamartoma of tuber cinereum	66
1.6.13 Chiasma opticum and hypothalamic glioma	66
1.6.14 Germinoma and teratoma	67
1.6.15 Dermoid and epidermoid.	67
1.6.16 Metastases	67
1.7 Diabetes insipidus	67
1.8 Syndrome of inappropriate secretion of ADH (SIADH)	72

2. THYROID GLAND	76
2.1 Embryological and anatomical remarks	76
2.2 Imaging methods	77
2.2.1 Ultrasonography	78
2.2.2 Computed tomography	79
2.2.3 Magnetic resonance imaging	81
2.2.4 Radionuclide imaging	82
2.2.5 Fine needle aspiration	84
2.2.6 Normal thyroid gland	85
2.2.7 Developmental abnormalities	86
2.3 Pathology	86
2.3.1 Nontoxic goiter	86
2.3.2 Diffuse nontoxic goiter	87
2.3.3 Nodular or multinodular goiter	87
2.3.4 Thyroid adenoma	89
2.3.5 Thyroid cysts	90
2.3.6 Intrathoracic goiter	91
2.3.7 Thyroid carcinoma	91
2.3.8 Imaging differential diagnosis of thyroid nodules	96
2.4 Hyperthyroidism	98
2.4.1 Diffuse toxic goiter – Graves-Basedow disease	100
2.4.2 Endocrine ophthalmopathy	102
2.4.3 Toxic adenoma, multinodular toxic goiter – Plummer disease	105
2.4.4 De Quervain thyroiditis – subacute thyroiditis	105
2.4.5 Painless thyroiditis	106
2.4.6 Iatrogenic causes of hyperthyroidism	106
2.4.7 Amiodarone thyrotoxicosis	106
2.4.8 Thyrotoxic crisis	106
2.5 Hypothyroidism	107
2.5.1 Myxedema coma	109
2.6 Thyroiditis	110
2.6.1 Autoimmune thyroiditis	110
2.6.2 Subacute thyroiditis	113
2.6.3 Silent thyroiditis	113
2.6.4 Postpartum thyroiditis	113
2.6.5 Suppurative thyroiditis	114
2.6.6 Riedel's thyroiditis	114
2.6.7 Radiation thyroiditis	114
2.6.8 Granulomatous diseases	114
3. ADRENAL GLANDS	116
3.1 Embryological remarks	116
3.2 Anatomical remarks	116
3.3 Imaging of adrenal glands	117
3.3.1 Plain X-ray of abdomen	118
3.3.2 Ultrasonography	118
3.3.3 Computed tomography	119
3.3.4 Magnetic resonance imaging	120
3.3.5 Angiography	120
3.3.6 Radionuclide methods	122
3.3.7 Adrenal biopsy	124

3.3.8 Normal adrenal gland	125
3.3.9 Imaging pitfalls	125
3.4 Cushing's syndrome – hypercortisolism	125
3.5 Primary hyperaldosteronism (Conn's syndrome)	134
3.6 Imaging of other adrenal pathology	135
3.6.1 Adrenal hyperplasia	135
3.6.2 Congenital adrenal hyperplasia	136
3.6.3 Infection and inflammation	136
3.6.4 Adrenal adenoma – differential diagnosis	137
3.6.5 Adrenocortical carcinoma	139
3.6.6 Adrenal hemorrhage	140
3.6.7 Adrenal cysts	140
3.6.8 Myelolipoma	141
3.6.9 Adrenal gland metastases	142
3.6.10 Adrenal hypoplasia and atrophy	142
3.7 Adrenal insufficiency – Addison's disease	142
3.8 Adrenal medullary tumors and paragangliomas	146
3.8.1 Pheochromocytoma	147
3.8.2 Neuroblastoma	151
3.8.3 Ganglioneuroma and ganglioneuroblastoma	152
3.9 Incidentaloma	152
3.10 Imaging remarks to differential diagnosis	155
4. GENITAL SYSTEMS AND SEX HORMONES	159
4.1 Embryological remarks	159
4.2 Disorders of sexual differentiation	159
4.3 Imaging	161
4.4 Female genitalia and hormonal disorders	161
4.4.1 Anatomical remarks	161
4.4.2 Female hypogonadism	162
4.4.3 Female infertility	169
4.4.4 Cystic pelvic mass	171
4.4.5 Functioning tumors and tumor-like ovary conditions	172
4.4.6 Polycystic ovary syndrome	173
4.4.7 Hyperandrogenism and hirsutism	175
4.4.8 Pelvic mass	177
4.5 Male genitalia and hormonal disorders	179
4.5.1 Anatomical remarks	179
4.5.2 Male hypogonadism	180
4.6 Other testicular disorders and imaging	185
4.7 Erectile dysfunction	193
4.8 Gynaecomastia	194
5. PARATHYROID GLANDS AND CALCIUM DISORDERS	196
5.1 Embryological and anatomical remarks	196
5.2 Imaging of parathyroid gland abnormalities	197
5.3 Hyperparathyroidism and hypercalcemia	197
5.4 Hypoparathyroidism and hypocalcemia	207
5.5 Extraskelatal calcifications and ossifications	210
5.6 Thymus and endocrine disorders	212

6. OSTEOPOROSIS AND SOME OTHER OSTEOPATHIES	215
6.1 Osteoporosis	215
6.1.1 Postmenopausal osteoporosis	217
6.1.2 Senile osteoporosis	218
6.1.3 Endocrine causes of osteoporosis	218
6.1.4 Osteoporosis in males	219
6.1.5 Other causes of osteoporosis	219
6.1.6 Diagnosis	221
6.1.7 Vertebral fractures	228
6.1.8 Therapy for osteoporosis	233
6.2 Osteomalacia	235
6.3 Renal osteodystrophy	238
6.3.1 Congenital renal osteodystrophy	240
6.3.2 Bone disease after organ transplantation	240
6.4 Osteitis deformans (Paget's disease)	240
6.5 Hypophosphatasia	243
7. PANCREAS AND NEUROENDOCRINE TUMORS	245
7.1 Development and anatomical remarks	245
7.2 Pancreatic neuroendocrine tumors	246
7.2.1 Insulinoma	249
7.2.2 Gastrinoma	251
7.2.3 Glucagonoma	252
7.2.4 Vasoactive intestinal peptide tumor – polypeptidoma	253
7.2.5 Somatostatinoma	253
7.2.6 ACTH-secreting tumors	254
7.2.7 Nonfunctioning islet cell tumor	254
7.3 Carcinoid	255
8. MULTIPLE ENDOCRINE NEOPLASIA	259
8.1 Multiple endocrine neoplasia syndrome type 1 (MEN 1)	259
8.1.1 Parathyroid tumors in MEN 1	260
8.1.2 Gastrointestinal neuroendocrine tumors	261
8.1.3 Vasoactive intestinal polypeptide tumor – polypeptidoma	263
8.1.4 Nonfunctioning islet tumors	263
8.1.5 Pituitary tumors	263
8.1.6 Carcinoid	264
8.1.7 Adrenal pathology	264
8.1.8 Less common manifestations of MEN 1	265
8.2 Multiple endocrine neoplasia syndrome type 2	265
8.2.1 Medullary thyroid carcinoma	266
8.2.2 Pheochromocytoma	266
9. ENDOCRINE HYPERTENSION	268
9.1 Pheochromocytoma and extraadrenal paragangliomas	269
9.2 Mineralocorticoid induced hypertension	275
9.3 Other endocrine causes of hypertension	278
10. DIABETES MELLITUS	285
10.1 Diabetes mellitus classification	285
10.2 Diagnostic criteria of diabetes mellitus	286

10.3 Principles of therapy	286
10.4 Diabetes mellitus complications	287
10.4.1 Diabetic coma	287
10.4.2 Microvascular complications	288
10.4.3 Macrovascular complications	290
10.5 Imaging of diabetes mellitus complications	296
10.6 Bone and joint complications	301
10.7 Urogenital complications	306
10.7.1 Diabetic nephropathy	306
10.7.2 Urogenital infection and inflammatory disorders	306
10.7.3 Imaging of urogenital complications	306
10.8 Other infections in diabetic patients	307
10.8.1 Malignant external otitis	308
10.8.2 Rhinocerebral mucormycosis	309
10.8.3 Acute necrotizing fasciitis	309
10.9 Diabetes mellitus and other endocrine diseases	309
10.9.1 Endocrine diseases with a diabetogenic effect	309
10.9.2 Autoimmunity in association with diabetes and other endocrinopathies	312
10.9.3 Effects of diabetes on endocrine function	313
10.10 Endocrine obesity	315
10.10.1 Endocrine function of the adipose tissue	315
10.10.2 Genetic causes of obesity associated with hypogonadotropic hypogonadism	316
10.10.3 Endocrine causes of obesity	316
10.10.4 The effect of obesity on endocrine functions	317
10.10.5 Imaging of obesity complications and body composition	318
10.10.6 Therapy of obesity	321
Color Figures	323
References	325
Abbreviations	339
Index	343

Preface

Over the past few years, endocrinology has belonged among the most dynamically developing clinical disciplines. At the same time, we are witnessing the rapid development of new diagnostic and therapeutic procedures which are increasingly dependent on the results of imaging methods. Currently there are many monographs and textbooks available which generally examine the clinical subjects only from the viewpoint of an expert in the given field. This monograph is unique in that it excludes this one-sidedness; by combining the experience of a diagnostic radiologist with a clinical endocrinologist, this publication achieves an entirely different dimension.

This monograph is the work of leading Czech specialists in the areas of radiology and endocrinology who have extensive clinical experience with the described endocrinopathies. What makes this comprehensible publication exceptional is the fact that it not only presents the clinical view of the endocrinologist on the various covered subjects, but the reader is also given the opportunity to learn about current diagnostic trends using imaging methods. This interdisciplinary view offers the reader a comprehensive insight into the field and the necessary knowledge for their clinical practice.

I am convinced that this book provides valuable information not only for medical students, endocrinologists and radiologists, but also physicians in other medical specialties. It will certainly become a useful aid in the everyday care of patients with endocrine gland diseases.

In Prague, July 20, 2012

Prof. MUDr. Petr Vlček, CSc.

Introduction

This manuscript, *Clinical Endocrinology and Diagnostic Imaging*, is based on our extended experience and pedagogical activity in the field of clinical endocrinology and imaging methods, as well as on our clinical research, literature, and published news. We have focused mainly on the information that could be relevant for the management of endocrine patient in day-to-day practice at endocrine and imaging clinics and departments. Diagnostic imaging and intervention methods as well as endocrinology have become multidisciplinary medical specialties with accelerated progress in recent years. About thirty years ago, we took part in introducing some new imaging methods (duplex Doppler ultrasonography, computed tomography, magnetic resonance imaging) in clinical practice in the Czech Republic as well as abroad, and the developments made by new technologies since then are substantial. To our knowledge, this is the first published monograph on the subject of imaging in endocrinology.

The diagnostic and differential diagnostic data of various endocrinopathies, both clinical and imaging methods are summarized in tables to facilitate their evaluation. We present laboratory results and reference values and their ranges in conventional units (weight per volume) used in the USA and also in SI units (mole per liter) widely used in Europe and other parts of the world. Radiation and radioactivity are presented in traditional and SI units as well (rad/gray, rem/sievert; curie/ becquerel) and their conversion factors are summarized in chapter Thyroid gland imaging. The ranges of normal reference of hormone and drug values may slightly differ in some working places and laboratories. There may also be individual variations including day-to-day variations and variations over the course of hours of hormone secretion and in relation to the physiology of the subject, including obesity, pregnancy, and exercise.

The chapter on therapy presents proven generic drugs and principles of management strategy for particular endocrine disorders. Therapy requires accurate diagnosis and detailed knowledge of the patient because no drug generates the same therapeutic effects on each person. Readers are encouraged to confirm the information about new drugs contained herein with other sources.

This monograph is intended not only for pre-graduate and post-graduate students but also for all young colleagues interested in clinical endocrinology and diagnostic imaging. We are aware that this manuscript does not and cannot cover all the details of the art of endocrinology, but even so have tried to present a wide variety of endocrine diseases with an emphasis on clinical use.

Ars longa, vita brevis.

Acknowledgement

We would like to acknowledge the input of Dr. Radek Pádr, Senior Consultant, Department of Radiology, Charles University in Prague, for most of the presented interventions, Prof. Dr. Petr Vlček, CSc., Head of the Department of Endocrinology and Nuclear Medicine, Charles University in Prague, and Prof. Dr. Karel Benda, DrSc., Professor of Radiology, Masaryk University Brno, for their review of the manuscript and constructive comments.

Prague, December 2011

J. Brunová, J. Bruna

1. Pituitary Gland

1.1 Embryology remarks

Pituitary gland (hypophysis) is formed from two sources during first eight weeks of fetal life. The **epithelial distal part** of the pituitary gland (adenohypophysis), which includes the pars anterior, pars intermedia, and pars tuberalis, originates from the primitive stomatodeal ectoderm called **Rathke's pouch**. The anterior wall of the

proximal portion of Rathke's pouch grows faster and forms distal part of the pituitary (adenohypophysis). The proximal portion of Rathke's pouch closes early but a remnant often persists into postnatal life as a cleft or residual basipharyngeal canal that lies between the distal part and neural part. Occasionally Rathke's pouch gives rise to a cyst, and later in postnatal life to a tumor (Fig. 1.1).

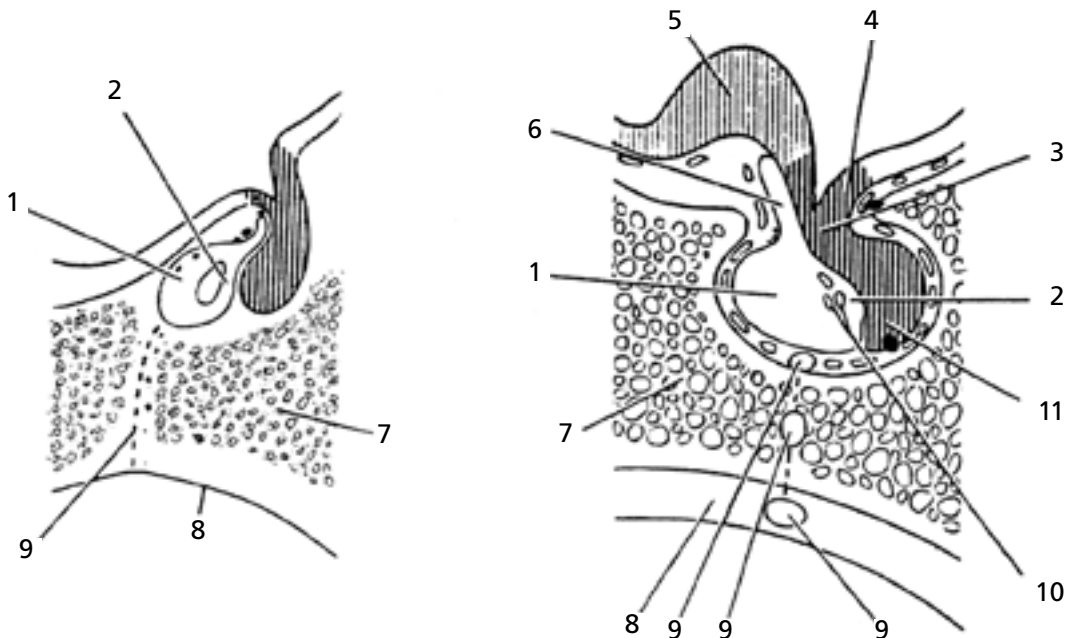


Fig. 1.1 Diagram of pituitary development – midsagittal section of the hypothalamus. 1 – anterior pituitary (adenohypophysis), 2 – pars intermedia of pituitary, 3 – infundibulum (pituitary stalk), 4 – foundation of eminentia medialis, 5 – chiasma opticum, 6 – anterior part of infundibulum, 7 – foundation of the sphenoid bone, 8 – upper pharynx, 9 – residual cranio-pharyngeal (base-pharyngeal) canal, a possible locations of accessory adenohypophysis, 10 – colloid deposits, 11 – posterior pituitary (neurohypophysis)

The neural portion originates from neuroectoderm of the diencephalon, includes infundibulum (pars infundibularis), neural stalk, and neurohypophysis (posterior pituitary), which adheres with pars intermedia of adenohypophysis (Fig. 1.1).

Histologic differentiation:

- *Acidophilic (eosinophilic) cells* = α cells are noticeable at about the third month of fetal life and produce growth hormone (GH) = somatotropin (STH) and lactogenic hormone prolactin (PRL).
- *Basophilic cells* = β cells appear a little later and are responsible for the secretion of corticotropin = adrenocorticotropin hormone (ACTH), thyrotropin = thyroid-stimulating hormone (TSH), follicle-stimulating hormone (FSH), luteinizing hormone (LH), interstitial-cell-stimulating hormone (ICSH) and melanocyte-stimulating hormone (MSH).
- *Chromophobe cells adenomas* are associated with hypopituitarism but may secrete prolactin, TSH and GH.

Pituitary hormones are synthesized early: The growth hormone and adrenocorticotropin hormone can be demonstrated at about the 9th week of gestation, and are followed by the appearance of glycoprotein hormones: a thyroid-stimulating hormone, a follicle-stimulating hormone, and a luteinizing hormone. Hormones of neurohypophysis, vasopressin = antidiuretic hormone (ADH) and oxytocin are synthesized in the hypothalamus and are found at about the 10th week of gestation. The neurosecretory material in the posterior lobe can be recognized at about the 20th week of gestation.

1.2 Anatomy remarks

The sellar region is a complex area composed of the bony sella turcica, pituitary gland, and adjacent structures (Fig. 1.2–1.4).

Bony sella. The bony sella turcica (pituitary fossa) is a cup-shaped depression in the central sphenoid bone that contains the pituitary gland and inferior part of the infundibular stalk.

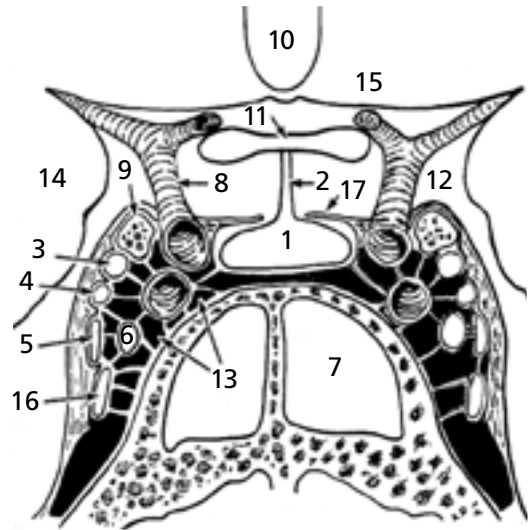


Fig. 1.2 Diagram of the sellar and parasellar structures in a coronal image. 1 – pituitary gland, 2 – pituitary stalk, 3 – nervus oculomotorius, 4 – n. trochlearis, 5 – ophthalmic branch of the n. trigeminus, 6 – n. abducens, 7 – sphenoidal sinus, 8 – arteria carotis interna, 9 – anterior clinoid processus, 10 – third ventricle, 11 – chiasma opticum, 12 – cistern suprasellaris, 13 – venous space of the cavernous sinus, 14 – medial wall of the middle fossa cranialis, 15 – hypothalamus, 16 – maxillary branch of the n. trigeminus, 17 – diaphragma sellae (according to AG Osborn, Diagnostic neuroradiology, Mosby – St. Louis 1994)

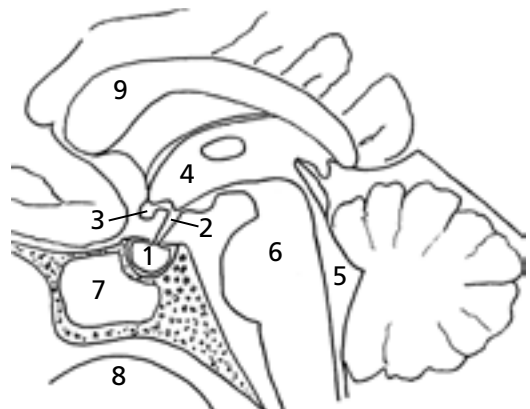


Fig. 1.3 Diagram of the pituitary and surrounding structures in the midsagittal section. 1 – pituitary gland, 2 – pituitary stalk (infundibulum), 3 – chiasma opticum, 4 – third ventricle, 5 – fourth ventricle, 6 – pons Varoli (pont), 7 – sphenoid sinus, 8 – space of the epipharynx, 9 – corpus callosum

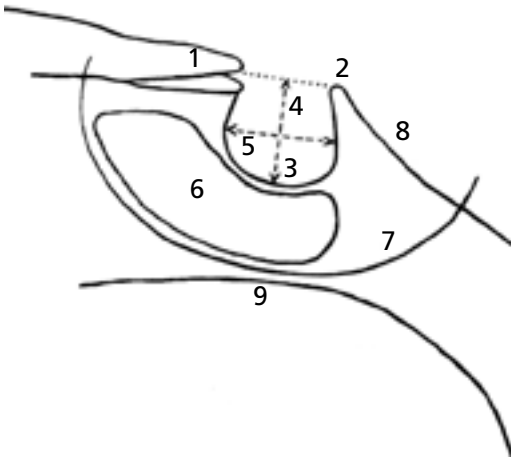


Fig. 1.4 Bony fossa measurement. 1 – anterior clinoid processes, anterior processes of the sphenoid bone (processes allae parvae ossis sphenoidaei), 2 – posterior clinoid process (dorsum sellae processus), 3 – bottom of the sella, 4 – depth of the sella – vertical diameters of the sella, 5 – length of the sella – ventrodorsal diameter of the sella, 6 – sphenoid bone sinus, 7 – bottom of the middle fossa of the skull base, 8 – clivus, 9 – space of the pharynx

The pituitary gland. The pituitary gland lies in the sella at the base of the brain in the central part of the middle cranial fossa. Lateral aspects of the pituitary gland are close to the cavernous sinus, medial wall of internal carotid artery, and the oculomotor, trochlear, and abducent nerves. The pituitary gland is composed of two lobes – anterior pituitary (adenohypophysis) and posterior pituitary (neurohypophysis). The pituitary gland is oval in shape, bilaterally symmetric with diameters about 13 mm (8–16 mm) transversally (width, latero-lateral diameter), \approx 12 mm (9–14 mm) antero-posteriorly (length, ventro-dorsal diameter) and \approx 6 mm (female 4–10 mm, male 3–7 mm) vertically (height, cranio-caudal diameter).

The volume of the pituitary gland is usually calculated as:

$$V = \frac{1}{2} \times \text{length} \times \text{height} \times \text{width}$$

or from the formula for an ellipsoid:

$$V = a \times b^2 \times \pi/6 \quad (a = \text{longer diameter})$$

The average weight of the pituitary gland is 0.6 g (0.4–0.8 g) in adults and 0.1 g at birth.

An increase in weight occurs during puberty, pregnancy and lactation, and a reduction in old age. In multiparous women, the pituitary gland weighs somewhat more than in nulliparous women or in men.

Note: In our study of adult people with growth failure due to primary pituitary dwarfism we also measured the volume of the pituitary gland on MR images in a reference group of 16 normal adult subjects without any pituitary and growth problems (age 42.9 years). Results have confirmed a relatively wide variation of pituitary size. The largest diameter of pituitary gland was transverse diameter – width 13.3 mm (10–14 mm), followed by sagittal diameter – length 12.1 mm (9–13 mm) and vertical diameter – height 6.2 mm (5–9 mm). The average volume of the pituitary gland in normal subjects was 654 mm³ (270–914 mm³) (Bruna, Brunova, 2002).

The anterior lobe (adenohypophysis) constitutes about 80% of the pituitary gland and can be divided into the following three parts:

1. Pars tuberalis (functionally associated with part of the infundibular stalk and median eminence of the hypothalamus)
2. Pars intermedia
3. Pars distalis

The posterior lobe, infundibular stalk, median eminence and supraoptic and paraventricular hypothalamic nuclei functionally belong to neurohypophysis.

The pituitary gland is covered by dura. The connective tissue of dura mater covering superior surface of pituitary is called sella diaphragm and has a small central opening 5 mm in diameter, which is penetrated by the hypophysial stalk. Above the sella diaphragm is suprasellar cistern, optic chiasm, median eminence, hypothalamus, and the third ventricle.

The **pars distalis** of pituitary gland is the main site of adeno-hypophysial hormone synthesis and discharge. The pars intermedium is rudimentary and its functional significance is in secretion of melanocyte-stimulating hormone. The pars tuberalis contains gonadotropes and thyrotropes.

The pituitary cells have a definite topographic representation within the gland. The prolactin and growth hormone secreting cells tend to be located predominate laterally, ACTH, TSH, FSH and LH secreting cells are located centrally. The secretion of these hormones is mediated by hormone-releasing factors produced in the hypothalamus and released into the hypophyseal portal system.

Normal variations of the anterior lobe

The shape, size, and signal intensity of the normal anterior lobe on MRI vary with the age, sex, and physiologic state of the individual. The pituitary gland of the neonate has a convex superior margin. Unlike the pituitary in an adult, the anterior lobe in the neonate has a homogeneously high signal on T1-weighted images. This appearance reflects the intense hormonal activity that begins during fetal life and continues into the neonatal period.

By two months of age, the convexity of the superior margin of the gland flattens out, the signal intensity of the anterior lobe decreases, and the anterior lobe can be clearly discriminated from the bright spot of the posterior lobe. The gland may have a slightly concave superior margin throughout childhood but is not expected to reach a height of greater than 6 mm (measured on the midline sagittal image). The pituitary stalk diameter is approximately 2 mm and never should exceed the diameter of the basilar artery.

At puberty, the gland increases in size, reflecting a period of high hormonal activity. At this time, gender variation is noted. The height of the gland in males reaches a maximum of 8 mm. In females, the gland may become markedly convex in superior contour and reach 10 mm in height. Hormonal activity in puberty is not as intense as occurs in the neonatal period, and there is no concurrent increase in signal of the gland as in neonates. In children with central precocious puberty, the gland increases in height and obtains the convex superior border seen at the time of normal

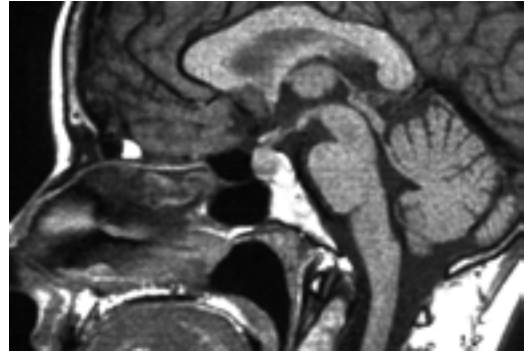


Fig. 1.5 Pituitary enlargement. Sagittal postcontrast T1GE image shows an enlarged pituitary gland in a pregnant patient

puberty. Following adolescence, the pituitary gland slowly decreases in size. With the exception of pregnancy, the pituitary gland remains relatively stable in appearance for most of adult life (Fig. 1.5). There is a gradual involution of the gland starting at approximately 50 years of age. But in women, a slight increase in height of the gland can be visible in the age of 50 to 59 years. It is suggested that this represents a compensatory gonadotropes hypertrophy responding to increased gonadotropin-releasing hormone (GnRH) resulting from a decreased feedback of circulating gonadal steroids. The hypertrophy of the gland during pregnancy and breast feeding is reflected on imaging as well (Fig. 1.6, 1.7). The gland obtains a markedly convex superior margin and increases in height up to 10 mm and the signal intensity of anterior lobe increases, too. This is presumably related to the same factors accounting for the hyperintense signal of the anterior lobe in neonates. This high signal persists into the immediate postpartum period, when the gland may reach a height as great as 12 mm. The pituitary stalk may increase in size but should not exceed 4 mm in diameter. During the second postpartum week the pituitary gland returns to its normal adult appearance.

Changes of the height and appearance of the pituitary gland may also be seen in patients with psychiatric nutritional problems.

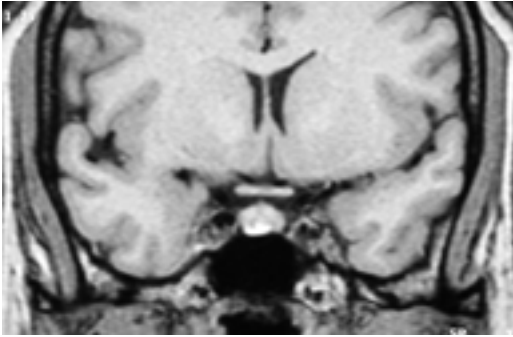


Fig. 1.6 Pituitary hyperplasia. Coronal MR T1 image of the pituitary region shows a diffuse enlarged pituitary gland with an area of hyperintensity from the floor – probably bleeding. Breastfeeding female 31 years old

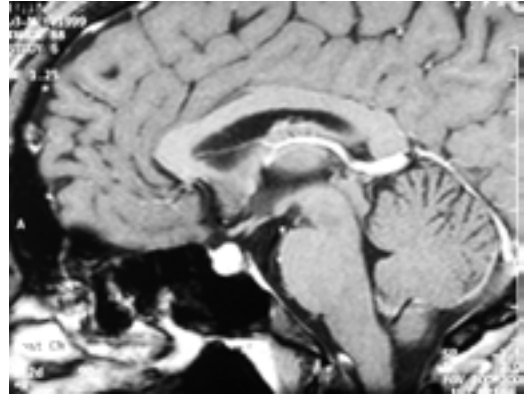


Fig. 1.7 Pituitary hyperplasia. Sagittal post-gadolinium MR T1 image of the pituitary region shows a diffuse homogenous enhancement of the enlarged pituitary gland. Breastfeeding female 31 years old

Adjacent structures

The suprasellar subarachnoid space lies above the sella diaphragm and is surrounded by the circle of Willis. The suprasellar cistern contains the optic nerves and chiasm and the upper part the infundibular stalk. The hypothalamus and anterior part of the third ventricle (optic recessus and pituitary recessus) are located just above the stalk.

Laterally, sella turcica is bordered by thin medial dural reflection of the cavernous sinus. The cavernous sinus is a multiseptated venous channel that contains the cavernous part of internal carotid arteries and cranial nerves: III – n. oculomotorius, IV – n. trochlearis, V – n. trigeminus (two branches: V1 – ophthalmic and V2 – maxillaris), and VI – n. abducens (see Fig. 1.2).

The sphenoid sinus occurs directly below the sella. Anteriorly, the sella floor is continuous with the tuberculum sellae and limbus sphenoidale. The dorsum of sella demarcates the posterior border of sella.

The cavernous sinus is best visible on coronal postcontrast CT and MR images or on magnetic resonance angiograms.

Blood supply

Main arteries supplying pituitary gland are the *superior and inferior hypophyseal arteries*.

Both of them arise from the internal carotid arteries. The inferior hypophyseal artery originates more proximally from the infraclinoid portion of the internal carotid artery and the superior hypophyseal artery more distally from the supraclinoid part of the internal carotid artery. The superior hypophyseal arteries penetrate the infundibulum and terminate in the primary capillary bed of the hypophyseal portal system. The portal vessels run along the infundibulum and terminate in the sinusoids of the secondary capillary bed. The adenohypophysis does not have a direct arterial supply. It receives its blood from the hypophyseal-portal system, which also serves as the pathway by which hypothalamic releasing hormones reach these structures. The inferior hypophyseal arteries, branches of the cavernous portion of the internal cerebral artery, carry blood to the neurohypophysis (Fig. 1.8).

Venous blood is transported from the pituitary by neighboring venous sinuses – cavernous sinus and petrosal sinuses to the jugular veins.

Innervation

The adenohypophysis has no direct nerve supply, expect for a few sympathetic nerve fibers that penetrate the anterior lobe along the

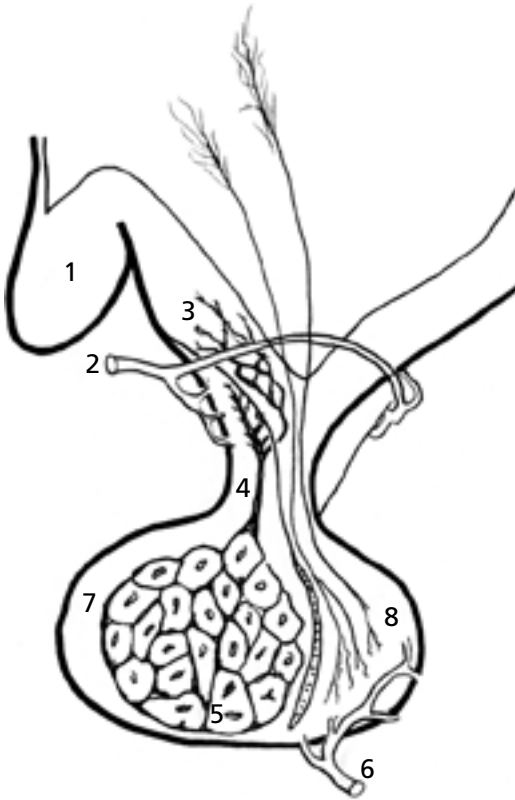


Fig. 1.8 Diagram of the vascular system of the pituitary gland – detail. 1 – chiasma opticum, 2 – a. hypophysialis superior, 3 – pituitary primary portal system, 4 – v. hypophysialis longa, 5 – pituitary secondary portal system, 6 – a. hypophysialis inferior, 7 – anterior pituitary – adenohypophysis, 8 – posterior pituitary – neurohypophysis (according to Tindall et al: Disorders of the pituitary, CV Mosby, St. Louis 1986)

vessels. The nerve fibers may affect adenohypophyseal blood flow but play no direct role in the regulation of anterior pituitary hormone secretion. The regulatory role of the hypothalamus is neurohumoral. It is done by stimulating and inhibiting hormones (factor) produced in the hypothalamus, which are transported by the portal vessels to the adenohypophysis.

The posterior lobe is richly innervated through the hypophyseal stalk by the supraoptico-hypophyseal and tubero-hypophyseal tracts.

The supraoptico-hypophyseal tract transports the neurosecretory material along the nonmyelinated nerve fibers from the hypothalamus to the posterior lobe

1.3. Imaging of the pituitary region

Imaging of the pituitary gland, sellar and parasellar region and exact evaluation of the clinical and laboratory data is often crucial because different conditions of this region may present with similar clinical findings.

Imaging methods:

- Plain X-ray of skull
- Computed tomography (CT)
- Magnetic resonance imaging (MRI)
- Cerebral angiography
- Inferior petrosal venous sinus sampling (IPSS)

Plain X-ray of skull

Plain X-ray imaging was mainly used in the pituitary gland diagnosis before the introduction of CT and MR into clinical practice. At present X-ray of skull is usually performed from the other than pituitary imaging indications (skull anomaly, trauma, tumors – metastatic malignancy, myeloma and others). However, the examination may reveal an unexpected expansion in pituitary region or suspicious skeletal changes for example in acromegaly. X-ray offers the advantage of being a cheap and noninvasive method for evaluation of the *pituitary fossa* (synonyms: sella, hypophyseal fossa of sphenoid bone, sella Turcica, Turkish saddle) changes, adjacent sinuses and bony structures. They yield a certain amount of important information – size, cortical margin and shape of sella, bony erosion or compression, double contour of sella, sphenoid sinus changes, and calcifications in the region.

The sella has usually been evaluated on lateral X-ray image and less exactly by posterior-anterior axial or semi-axial Town's projection.

The **normal diameters** of the pituitary fossa on lateral plain X-ray can be slightly larger than the pituitary gland because of the fibrotic tis-

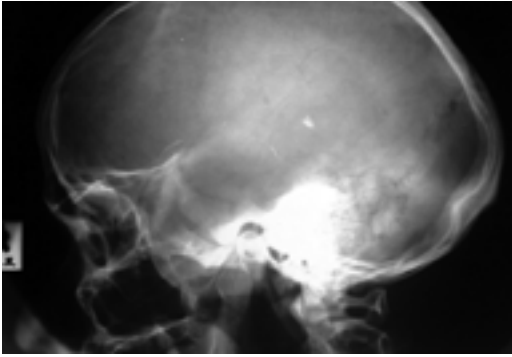


Fig. 1.9 Plain skull X-ray shows large expansion in the sella Turcica

sue, venous plexuses and subarachnoid space changes lying between the gland and bone. We have to take into consideration also possible projection magnification. The *length* of bony sella from anterior to posterior wall is about 12 mm (5 to 15 mm), the *depth* (vertical diameter from the line of the anterior sphenoidale processes – anterior clinoid processes – to the sella bottom) is about 6 mm (4 to 12 mm), the *width* of sella is about 12 mm (8–19 mm).

On lateral projection the pituitary fossa is a U-shaped structure with a dense cortical bone margin. Those parts of sella turcica that are outlined by underlying air spaces of the sphenoid sinus exhibit a thin cortical margin which is related to the lamina dura. The *planum sphenoidale* is a flat and thin bone partly form-

ing the roof of the sphenoid sinus. The planum sphenoidale expands posteriorly to terminate in the *anterior sphenoidale processes*. The chiasmatic sulcus in the planum sphenoidale ridge conforms to the optic chiasm and optic nerves. The inferio-posterior margin of the chiasmatic sulcus is the *tuberculum sellae*. The *floor* of the sella is not perfectly semicircular in shape but gives a more oval-shape image (see Fig. 1.4).

The *posteroanterior projection* of the sella turcica is less informative than the lateral one but may be useful in determination of the sphenoid sinus lateral margin and the floor of the sella turcica. The floor frequently bows slightly inferiorly.

The plain X-ray is usually able to detect major space occupying lesions; however, the variations of the shape of sella turcica do not always reflect the pathology of hypophysis and the adjacent structures (Fig. 1.9).

Computed tomography

Computed tomography (CT) was the first imaging method which allowed to demonstrate exact pituitary gland, hypothalamus, basal cisterns, optic nerves, and optic chiasm and to measure the organ density. CT is more sensitive than either plain radiography or magnetic resonance in imaging the bone structure changes and in detection of calcifications within soft tissues.

On CT images, pituitary gland is isodense to the gray matter of the brain (Fig. 1.10a, b).

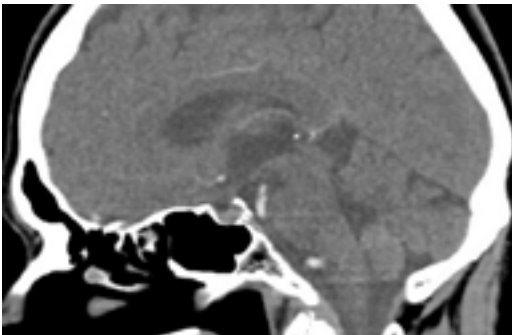


Fig. 1.10a CT image in sagittal reconstruction of a normal pituitary gland and sella

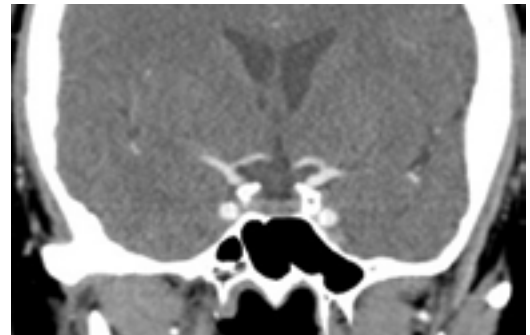


Fig. 1.10b Postcontrast coronal CT image of a normal pituitary gland in coronal reconstruction

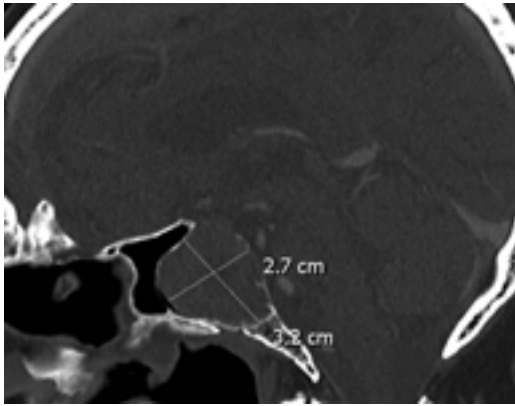


Fig. 1.11 Pituitary adenoma. Sagittal CT image demonstrates sellar expansion 3.2 x 2.7 cm with an invasion into the sphenoid sinus and occipital bone – clivus

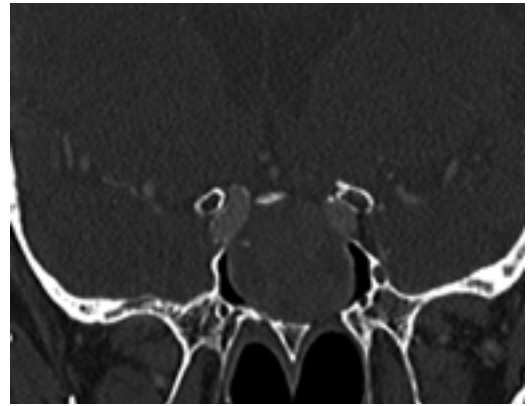


Fig. 1.12 Pituitary adenoma. Coronal CT image shows a large pituitary expansion invading the sphenoid sinus

The cerebrospinal fluid spaces are of lower density (0 to 10 Hounsfield units – HU), and fat structures exhibit much lower density than the cerebro-spinal fluid (–80 to –120 HU). The density of brain and pituitary gland is about 35 (30–40) HU. Thin slice CT technique (2–4 mm), high resolution CT-HRCT (1 mm slices) and postcontrast study are used in exact evaluation of the sella region (1–4 mm slices, 0.1 distance factor, FOV 200 mm). Intravenous injection of non-ionic or low osmolality iodine contrast agent (1 ml/1 kg of body weight, iodine concentration 300–350 mg/ml, osmolality 600–800 mOsm/kg) has been generally used in CT of brain. Plain CT of head including sella region remains basic imaging method for the detection of other than pituitary pathology: trauma, stroke, tumor and some neurologic problems (Fig. 1.11, 1.12).

After intravenous contrast agent, the blood vessels, cavernous sinus, pituitary gland and pituitary stalk all enhance intensely. Approximately 10 seconds after the enhancement of supraclinoid carotid arteries occurs, there may be visible focal enhancement localized just ventral to the stalk in the mid-anterior aspect of the pituitary gland called the “tuft”. Displacement or compression of the tuft (the “tuft sign”) was described as a secondary marker for pituitary pathology. The postcontrast

CT helps to define the pituitary gland and also the cranial nerves within the cavernous sinus.

A disadvantage of CT comprise radiation exposure, artifacts from X-ray beam hardening related to the dense bony skull base, and less than ideal soft tissue characterization. Additionally, on coronal images there are often artifacts from metallic dental fillings. In pituitary imaging CT was replaced by magnetic resonance imaging.

Magnetic resonance imaging

Magnetic resonance imaging (MRI) of pituitary gland currently represents the gold standard and method of choice in pituitary imaging. The MRI examination starts constantly with a pilot study (localizer) and we continue with axial T2W imaging of the whole brain to exclude pathologic changes from areas distant to the pituitary gland.

The standard protocol for evaluating the pituitary gland consists of pre-contrast and post-contrast thin slices through the sella in sagittal plane, and coronal planes using T1W sequences (Fig. 1.13).

We execute MRI of pituitary gland in thin slices (1–2 mm, distance factor 0.1, FOV 200 mm) in T1GE (GE – gradient echo) images or in

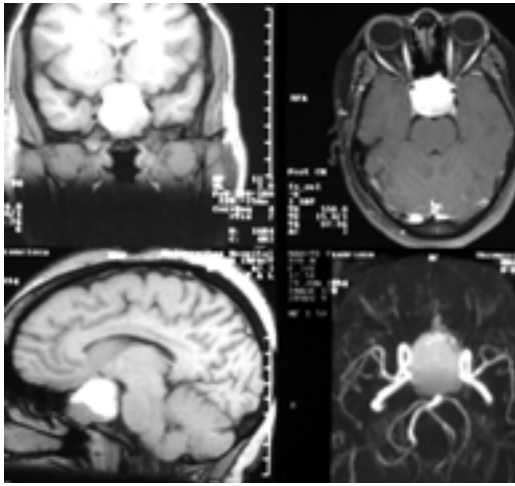


Fig. 1.13 Hypofunctioning macroadenoma. Female 30 years old with temporal hemianopsia, hyperprolactinemia. Postcontrast MR scan and MR angiography show a large complex mass in the intra- and suprasellar regions. Left: precontrast MRI, right: contrast MRI

T1SE images (TSE – turbo spin echo / FSE – fast spin echo) without contrast. The second study is performed in the same planes and in the same sequence immediately after the intravenous injection of contrast agent Gd-DTPA (gadolinium-diethylenetriamine pentaacetic acid) in the amount of 0.1 mmol per kilogram of body weight (0.1 mmol/kg). The 0.1 mmol of Gd-DTPA is equal to 0.2 ml of Gd-DTPA.

Gadolinium is a rare-earth heavy metal ion paramagnetic substance, which shortens T1 and also T2 relaxation time of hydrogen nuclei within its local magnetic field. The gadolinium significantly increases the signal intensity of T1 images and decreases only a little signal intensity of T2 images. Therefore T1 sequences are used on post-gadolinium studies. However, if gadolinium concentration in tissue is high, the loss of signal intensity is observed on T2W images, too.

The post-Gd-DTPA MR images enable to identify blood supply of the tissue, to determine regions with the disrupted blood-brain barrier, to enhance in vascularized tissues and therefore to accentuate pathology, and gener-

ally to evaluate the lesion with an increased enhancement.

The Gd-DTPA is excreted from the body by glomerular filtration. About 80% of intravenously injected Gd-DTPA is eliminated in 3 hours.

Adverse reaction on Gd-DTPA is uncommon. If any, it is minor and includes headache, nausea, local pain, and coldness.

Contraindication. Gadolinium is contraindicated in pregnancy and in breast feeding women.

Magnetic resonance characteristics of pituitary gland

Normal pituitary gland visible on MRI is composed of two different parts – larger anterior adenohypophysis and smaller posterior neurohypophysis. Both parts are homogenous on MR images but gives different MR signal. On pre-contrast T1 images, the pituitary gland appears as a crescent area of soft tissue along the floor of the sella. Majority of the gland visualized on MRI constitutes the *anterior lobe* (approximately 4/5 of gland) and its signal is equivalent to that of the gray matter. The adenohypophysis is isointense with white matter on T1 and T2W images. The smaller *posterior lobe* (neurohypophysis) is hyperintense on T1 images and usually appears as a “bright spot” at the posterior aspect of the sella due to phospholipid content in neurosecretory granules bearing vasopressin. The posterior pituitary is best seen on midline sagittal slices (Fig. 1.14).

Pars intermedia of pituitary gland is not demarcated and therefore is not distinguishable on images made with any imaging techniques.

The *pituitary stalk* (infundibulum) joins the posterior lobe at the junction of the anterior and posterior lobes. The *infundibulum* extends from the mid aspect on the top of the gland dorso-cranially towards the median eminence of the hypothalamus, coursing through the supra-sellar cistern. The infundibulum is seen extending vertically from the middle portion of the gland to the hypothalamus. The stalk is wider at the level of the hypothalamus and gradually

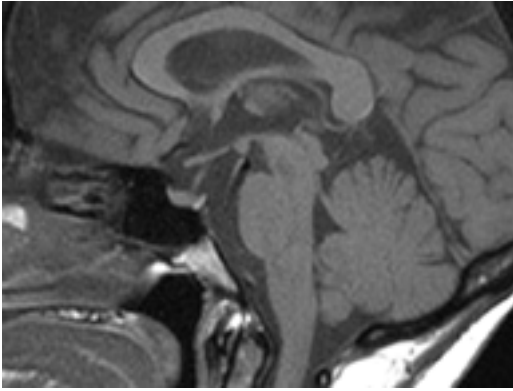


Fig. 1.14 Sagittal T1WI in midline demonstrates neurohypophysis as a “bright spot” in the typical location at the dorsal sella region

tapers in width as it joins the gland. The width of a normal infundibulum should not exceed 4 mm. *Other normal suprasellar structures*, such as the optic chiasm and optic nerves, third ventricle with pituitary and chiasm recessus, and mamillary bodies, are seen as well. On coronal images, the pituitary gland has a broad rectangular shape. The superior dural reflection, the diaphragma sellae, may also appear as a band of low-signal intensity in some cases.

The “bright spot” is related to the concentration of vasopressin stored in the posterior lobe.

Note: It is still not clear what is exactly responsible for the high signal. Two theories have been proposed. Oxytocin and vasopressin synthesized in the hypothalamus are linked to neurophysins, which are carrier proteins. This compound is then packed within phospholipid membranes to become the neurosecretory granules that are stored in the posterior lobe. The phospholipid membrane of the neurosecretory granules can be responsible for the high signal as well.

The absence of high signal in the neurohypophysis area is associated with central diabetes insipidus, severe dehydration in hyperosmolar (Fig. 1.15, 1.16) and ketoacidotic diabetic coma, and with compressive pituitary gland lesion. More details see in the chapter “Diabetes insipidus”.

On both sides of the gland lies the cavernous sinus with cavernous segment of the internal carotid arteries and cranial nerves. The lateral dural margin of the cavernous sinus is a thin linear structure of low signal. The pre-contrast signal of almost whole cavernous sinus except arteries is equivalent to that of the adjacent brain. Rapidly flowing blood presents as area without signal structure due to flow void effect. Therefore arteries are well-recognizable as a black round, ovoid or longitudinal structure lying centrally within cavernous sinus. Nonenhanced spots along the lateral wall of the cavernous sinus are *cranial nerves (CN)* and their topography is as follow: oculomotorius nerve (CN III) localized

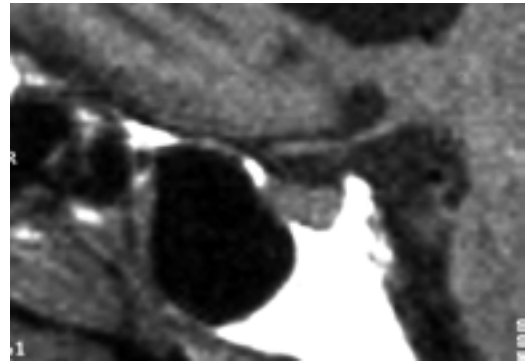


Fig. 1.15 Hyperosmolar coma. Sagittal plain T1GE image shows the loss of a “bright spot” of the neurohypophysis

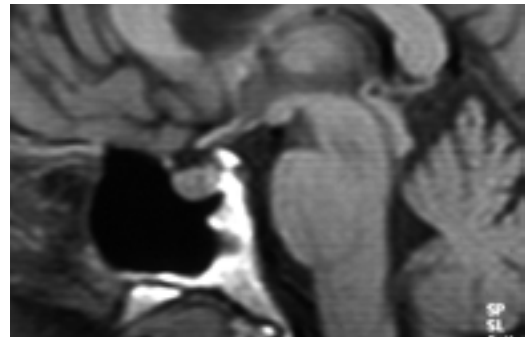


Fig. 1.16 Patient with central diabetes insipidus. Sagittal plain T1GE image shows an absent high signal of neurohypophysis and a “pseudo bright spot” above the pituitary gland produced by bony marrow in the enlarged dorsum sellae

superior and lateral, trochlearis nerve (CN IV) localized lateral, first branch of trigeminal nerve (CN V-1) localized inferior and lateral, and abducent nerve (CN VI) medial within the cavernous sinus (courses through this region towards the superior orbital fissure). The cranial nerves maintain a constant *anatomic relationship to the cavernous sinus*, dura and to each other (see Fig. 1.2). The maxillary branch of the trigeminal nerve (CN V-2) is inferior in position, located just below the cavernous sinus as it extends to the foramen rotundum.

Dynamic of the pituitary gland enhancement. Images performed after intravenous injection of a contrast agent show a homogenous enhancement of the gland and the adjacent cavernous sinus. Because of rapid blood flow, the carotid artery tends to remain black on MRI. The pattern and sequence of enhancement of the various portions of the pituitary gland mirror the circulation of arterial supply. The posterior lobe (neurohypophysis) expresses the earliest enhancement followed by enhancement of median eminence and the infundibulum. Finally, the anterior lobe begins to enhance starting at the junction of the anterior lobe with the infundibulum and then extending to the more peripheral portions of the lobe. Dynamic imaging is a technique whereby the acquisition of images occurs on a fast time scale synchronous with the microcirculation. Currently, it is believed that the infundibulum enhances approximately 4 seconds following enhancement of the posterior lobe and 10–15 seconds later is enhancement of the anterior lobe. An alteration in this sequence of enhancement may signify underlying pathology.

Increased signal intensity of pituitary gland.

On T1W images the high signal in dorsal part of pituitary gland corresponds to normal functioning posterior pituitary. Increased signal of adenohypophysis usually signalizes bleeding within the pituitary gland (pituitary apoplexy, Sheehan syndrome), but mainly hemorrhage into the pituitary macroadenoma, more rarely to carcinoma, or to pituitary metastases (melanoma, breast, lung, kidney, thyroid or choriocarcinoma).

Increased signal intensity of adenohypophysis (anterior pituitary) on T2W images can be a sign of tumor, bleeding, cyst, abscess, hepatic failure, lymphocytic hypophysitis.

Contraindications. The contraindications to MRI include patients with cardiac pacemaker, cerebral spring aneurysm clip and metallic foreign body near a vital structure, neural stimulators, and some other electronic and metal implants.

Contraindication for intravenous administration of Gd-DTPA is pregnancy, lactation and renal failure. Plain MRI without a contrast agent is not contraindicated but it is not recommended to perform a MR examination in the first trimester of pregnancy.

Cerebral angiography

Cerebral angiography is an important and the best imaging method for a detailed evaluation of all vascular structures and for intravascular interventional procedures (vessel dilatation, coiling, stent introduction). Indications for cerebral angiography were cut down significantly by introducing cross section 3D techniques, especially by clinical employing CT and MRI. Carotid angiography is a method of choice for diagnosis of extracranial vascular pathology, detail evaluation of vascular malformation and blood flow generally before any vascular surgery. The carotid angiography has been also established as a method of choice in diagnose of vascular parasympathetic paraganglioma in region of neck and head (Fig. 1.17–1.19).

Inferior petrosal venous sinus sampling

The inferior petrosal venous sinus sampling (IPSS) is a term used for the inferior petrosal venous sinus angiography with blood sampling. The IPSS is indicated for the detection of suspected ACTH secreting adenoma (Cushing's syndrome, resp. Cushing's disease) when the standard MR imaging failed to prove any pituitary lesion. With usual Seldinger's technique a thin catheter is placed into the inferior petrosal

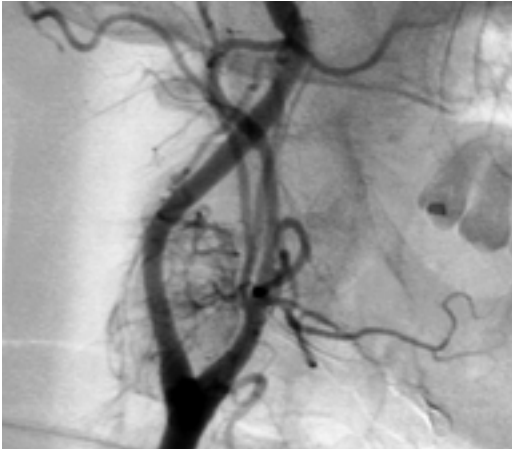


Fig. 1.17 Carotid body paraganglioma. Angiography of the right CCA shows a well demarcated hypervascularized lesion expanding carotid bifurcation

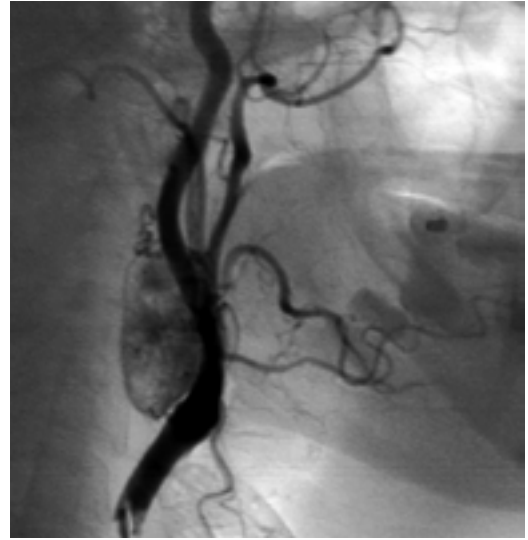


Fig. 1.18 Carotid body paraganglioma. Lateral view of CCA angiography shows a hypervascular lesion, which deviates bifurcation of the CA ventrally



Fig. 1.19 Carotid body paraganglioma after embolization. ECA angiography demonstrates deviation of the surrounding vessels and no more pathological vascularization

sinus and samples of venous blood are taken at exact time intervals. At first without any pituitary stimulation, the basal ACTH level are sampled and later samples are drawn after the administration of 100 µg corticotropin-releasing hormone (CRH) intravenously. The IPSS test has to be well prepared with the cooperation

with the endocrinologist, and performed by two simultaneously working experienced invasive radiologists. The hormone results of ACTH blood levels from IPSS have 95% sensitivity and 100% specificity if the ratio of central ACTH to periphery ACTH is > 2:1 and after stimulation > 3:1. For more details of IPSS see imaging of corticotropic pituitary adenoma.

1.4 Pituitary adenomas

Pituitary adenomas can be divided into hormonally active (functioning adenoma) or hormonally inactive (nonfunctioning adenoma). Most pituitary adenomas are functioning and patients present with endocrine hyperfunction. Non-functioning adenomas frequently go unnoticed until they are large enough to cause mass effect and/or multiple pituitary hormone deficiencies, even panhypopituitarism can occur owing to compression of the stalk of the residual pituitary (Fig. 1.20–1.23).

Adenomas are also categorized according to size, either small (microadenomas ≤ 10 mm) or large (macroadenomas > 10 mm).

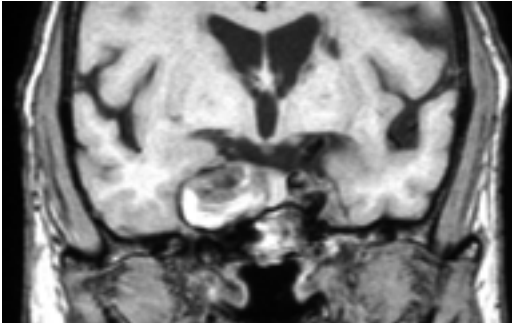


Fig. 1.20 Hyperprolactinemia. Coronal T1 image post Gd-DTPA shows MR aneurysm of the right ICA with compression of the pituitary gland (female 69 years)

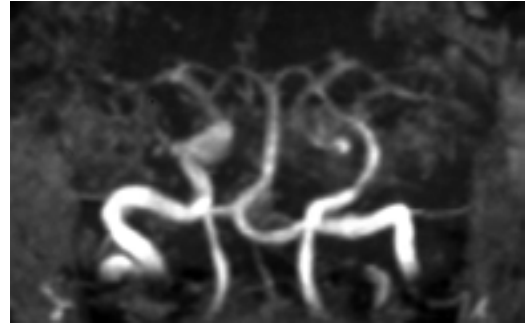


Fig. 1.21 Hyperprolactinemia. MR angiography shows a partly thrombolized aneurysm of the right ICA (female 69 years)

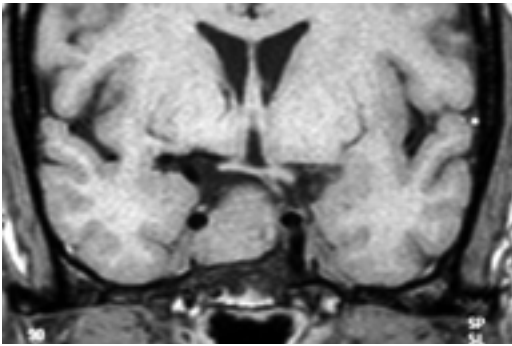


Fig. 1.22 Prolactinoma. Sagittal plain T1GE image shows homogeneous asymmetric pituitary expansion growing from the right part of the organ involving the cavernous sinus on the right side. Pituitary stalk is dislocated to the left side, optic chiasm partly compressed

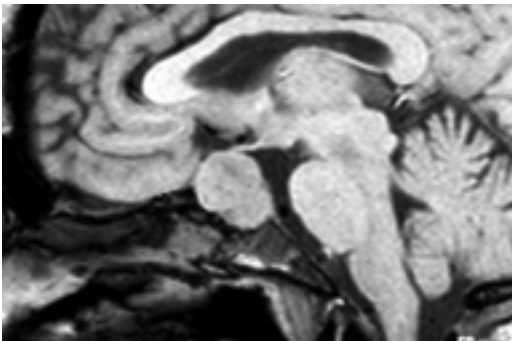


Fig. 1.23 Prolactinoma. Sagittal plain T1GE image shows not homogeneous pituitary gland expansion

Pituitary adenomas are benign and slowly growing neoplasm arising from adenohypophysis. They tend to be hypovascular in comparison with normal adenohypophysis. The MRI of pituitary adenomas follows their pathophysiology. Adenomas are slightly hypointense or isointense on T1W images and after intravenous injection of a contrast agent (Gd-DTPA) became more markedly hypointense in comparison with the postcontrast signal intensity of normal anterior pituitary and stalk, which are enhancing significantly due to the lack of blood-brain barrier. Small adenomas are generally homogenous and macroadenomas more frequently nonhomogenous in appearance. Functioning pituitary adenomas tend to be diagnosed in the early stages as microadenomas (diameter < 10 mm). However, nonfunctioning adenoma may reach an enormous size before the time of diagnosis. The shape of the microadenoma is round or ovoid, eventually lobulated. Multiple pituitary adenomas are rarer but not uncommon findings (Fig. 1.24, 1.25). The pituitary macroadenoma is usually a nonhomogenous and lobulated mass, compressing or infiltrating stalk, optic nerves and cavernous sinuses and causing mass effect: bitemporal hemianopsia, hypopituitarism, cranial nerve palsy (nn. oculomotorius, trochlearis and trigeminus) and even pituitary apoplexy (Fig. 1.26). Large macroadenomas may present with hydrocephalus or invasion into carotid artery.

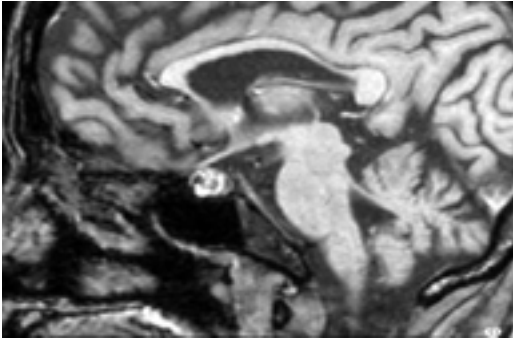


Fig. 1.24 Hyperprolactinemia. Plain sagittal T1GE image shows the enlarged pituitary with two hypointense lesions

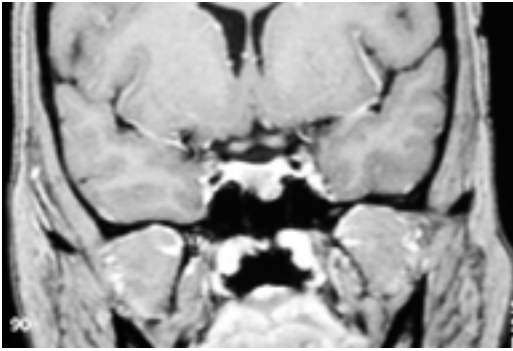


Fig. 1.25 Bilobulated prolactinoma. Coronal post-gadolinium MR T1 of the pituitary region image shows a bilobulated hypointense lesion. Female 31 years old with hyperprolactinemia

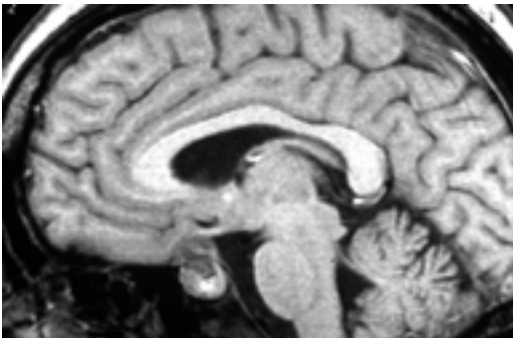


Fig. 1.26 Nonfunctioning pituitary adenoma. Sagittal plain T1GE image demonstrates large heterogeneous pituitary expansion with a small area bleeding inside. The expansion compressed the optic chiasm. Patient sent for MR with visual problems

Pituitary adenomas are by far the most common intrasellar and parasellar neoplasm in adults but they are rare in children. Only about 3% of adenomas occur before 18 years of age. The majority of pediatric pituitary tumors are detected in adolescent girls and they predominantly comprise prolactinomas and ACTH-secreting adenomas.

The asymptomatic and incidentally diagnosed pituitary mass is called pituitary incidentaloma (see Chapter 1.4.7).

Microadenomas

Adenomas measuring less than 10 mm in diameter are defined as microadenomas. These tumors are often localized within the sella and do not exhibit suprasellar extension. Most microadenomas are less vascularised compared to adeno-hypophysis and enhance less rapidly than the surrounding normal pituitary tissue. On plain CT and especially on MR T1WI microadenomas are slightly hypo- or isodense and hypo- or isointense respectively. On early postcontrast study they became significantly hypodense or hypointense, particularly if dynamic sequences are performed. Adenomas may show enhancement on delayed images due to the increased permeability of gadolinium and due to the decreased washout time (reverse enhancement). A focal bulge on the surface of the pituitary gland or a focal depression of the sella floor can be visible. Adenomas larger than 5 mm may compress or dislocate the pituitary stalk.

Hormonally active microadenoma becomes apparent clinically earlier and therefore it is diagnosed sooner than nonfunctioning adenoma. The majority of pituitary microadenomas comprise prolactinomas or corticotrophic adenomas.

Microadenoma is usually diagnosed on MRI as a round and nonenhancing mass hypointense on T1W and hyperintense on T2W images. On postcontrast (Gd-DTPA) T1W images, microadenoma is markedly hypointense in comparison with residual adeno-hypophysis. One third

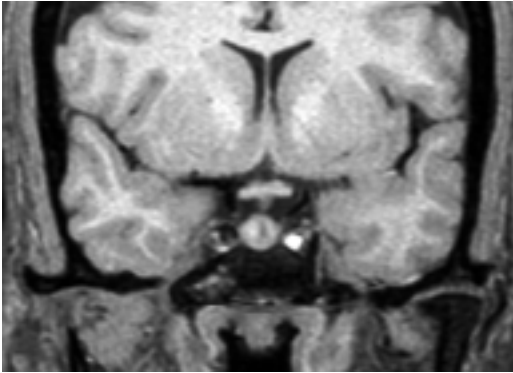


Fig. 1.27 Hyperprolactinemia. Coronal plain T1GE image demonstrates nonhomogenous enlargement of the adenohypophysis with hypointense and hyperintense spots – microadenoma of the pituitary

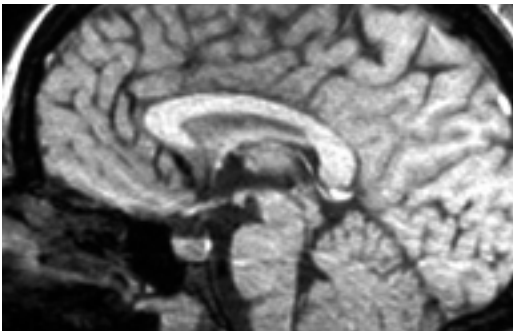


Fig. 1.28 Hyperprolactinemia – microprolactinoma. Sagittal plain T1GE image shows a small hypointense lesion at the bottom of the adenohypophysis

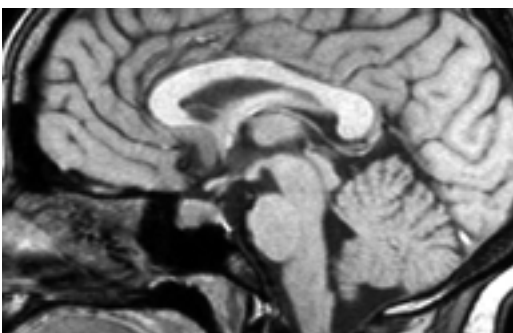


Fig. 1.29 Hyperprolactinemia – two microprolactinomas. Sagittal plain T1GE image shows two small hypointense lesions at the bottom of the adenohypophysis

of small lesions may be overlooked without gadolinium enhancement and one third of the lesions can be missed despite enhancement if the scanning is not performed immediately after Gd-DTPA injection (Fig. 1.27–1.29).

Macroadenomas

Adenomas equal to or larger than 10 mm in diameter are defined as macroadenomas. Macroadenomas are frequently hormonally inactive and represent about 70% of pituitary nonfunctioning adenomas. Macroadenomas are tumors of adult patients, diagnosed usually at the age of 25–60 years. There is no gender predominance.

The clinical symptoms arise mainly from mass effect of tumor: bitemporal hemianopsia, obstruction of foramen Monroe and hydrocephalus, hypopituitarism, cranial nerves III, IV and VI palsy.

Imaging

Plain X-ray film in lateral projection may demonstrate enlargement of sella, elevated anterior clinoid processes, double floor of sella, sella dorsum erosions. These changes usually herald large pituitary neoplasms.

Computed tomography images reveal pituitary fossa expansion with a mass generally isodense to the brain. The mass can be homogenous but often is nonhomogenous with areas of hypodensity (necrosis and cystic component) or hyperdensity (bleeding and rarely calcifications). The pituitary gland is upward convex, the height is more than 10 mm, pituitary stalk is compressed or deviated, floor of the pituitary fossa is very often eroded, and pituitary gland is asymmetric. The postcontrast study early images show low enhancement, but on late scan the enhancement can be visible.

On *magnetic resonance* images the macroadenomas are usually isointense to the gray matter and homogenous. The heterogeneity of the mass is a sign of necrotic degeneration or bleeding (Fig. 1.30–1.32). Cystic macroadenomas can give a different signal in their cystic compart-

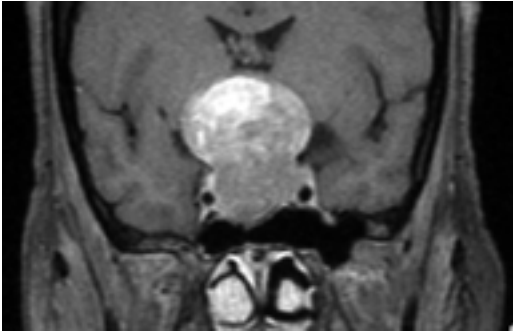


Fig. 1.30 Acromegaly. Coronal plain T1GE image demonstrates a large slightly hyperintense tumor expanding suprasellarly into the hypothalamus and third ventricle and with localized bleeding in the patient with anopsia and acromegaly

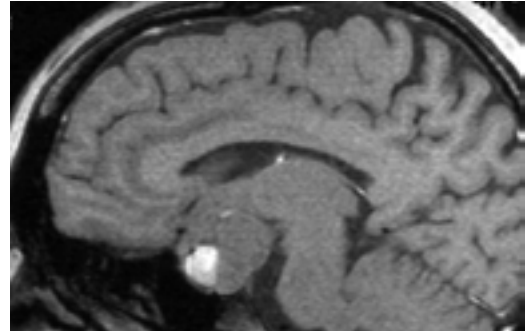


Fig. 1.31 Hyperprolactinemia. Plain sagittal MR T1GE image shows a large prolactinoma, which compresses the optic nerves, the third ventricle and the hypothalamus. Local hyperintensity in the adenoma corresponds to bleeding



Fig. 1.32 Prolactinoma. Plain coronal MR T1GE image shows pituitary macroadenoma compresses optic nerves, 3rd ventricle and hypothalamus on right side. Local hyperintensity in adenoma corresponds to bleeding

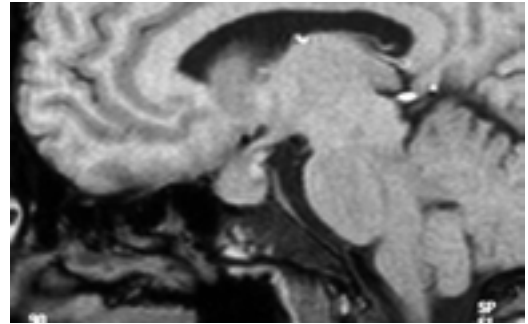


Fig. 1.33 Nonfunctioning pituitary adenoma. Plain sagittal T1GE scan shows a round sellar mass expanding suprasellarly. Pituitary stalk is compressed and posterior pituitary dislocated partly above the diaphragm

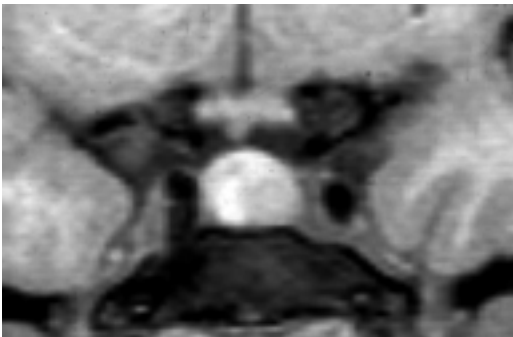


Fig. 1.34 Macroprolactinoma. Coronal plain T1GE image demonstrates nonhomogenous pituitary mass with two hypointense lesions, larger on the left bottom – functioning prolactinoma. The hyperintensity between the lesions conforms to a bleeding

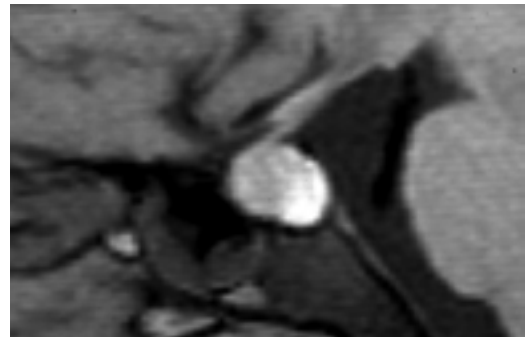


Fig. 1.35 Prolactinoma. Sagittal plain T1GE image shows nonhomogenous expansion with a hyperintense area of bleeding in the dorsal bottom part which slightly bulged into sphenoid bone

ment, which is dependent on the protein content of the cyst. The signal intensity of the adenoma with hemorrhage changes according to the hemoglobin degradation. Obviously, examination of the patient with acute and subacute hemorrhage reveals a high density on CT and shows a high intensity signal on T1W and T2W images. The noncomplicated adenoma usually gives a slightly lower signal intensity on T1-weighted images and slightly higher on T2, FLAIR and IR images in comparison with brain tissue and normal residual anterior pituitary tissue (Fig. 1.33–1.35).

A massive hemorrhage into the adenoma causes pituitary insufficiency (apoplexy of the pituitary gland). Hemorrhage is possible to confirm by CT or by MR imaging. After the onset of acute neurological symptoms the patient is at first examined by CT. Generally, the fresh acute bleeding is hyperdense 50–90 HU (1–7 days), late-subacute (second week after the attack) is isodense, and even later (after > 3 weeks) becomes hypodense.

MR images of hemorrhage:

- *hyperacute phase* (< 24 hours): isointense T1, hyperintense T2 (oxyhemoglobin)
- *acute phase* (1–3 days): hypointense T1, hypointense T2 (deoxyhemoglobin)
- *subacute early* (> 3 days): hyperintense T1, hypointense T2 (methemoglobin)
- *subacute late* (> 7 days): hyperintense T1, hyperintense T2 (methemoglobin after lysis of RBCs)
- *chronic* > 14 days): hypointense T1, hypointense T2 (hemosiderin)

The function of the pituitary gland may improve after the resorption of hematoma but usually hypopituitarism persists and pituitary size is significantly smaller.

The extension of macroadenomas into suprasellar cistern, cavernous sinus, sphenoid sinus and nasopharynx occurs in up to 70% of patients at the time of diagnosis. Occasionally, but not rarely, macroadenoma shows tumor hemorrhage, focal necrosis, invasion of sphenoid sinus, clivus and/or cavernous sinus with carotid artery encasement, expansion into the third and into lateral ventricles (Fig. 1.36–1.40).

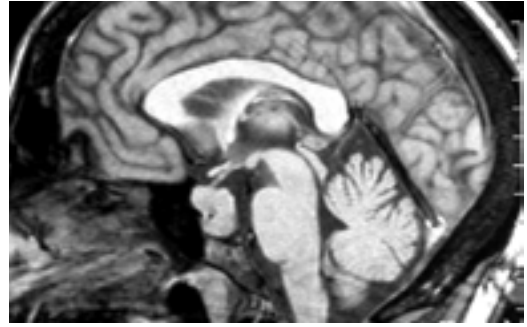


Fig. 1.36 Pituitary TSH-adenoma. Sagittal postcontrast T1GE image shows a pituitary tumor expanding with invasion of the occipital bone (clivus) and a slight protrusion into the sphenoid sinus

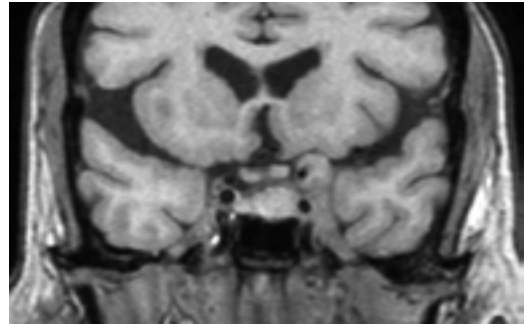


Fig. 1.37 Prolactinoma. Coronal plain T1GE image demonstrates macroadenoma of left part of the adenohypophysis expanding into the cavernous sinus

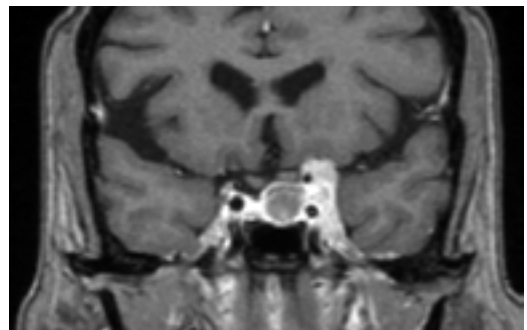


Fig. 1.38 Macroprolactinoma. Coronal postcontrast T1GE image demonstrates macroadenoma of the left part of the adenohypophysis with a multinodular invasion into the cavernous sinus and compression of the left optic nerve

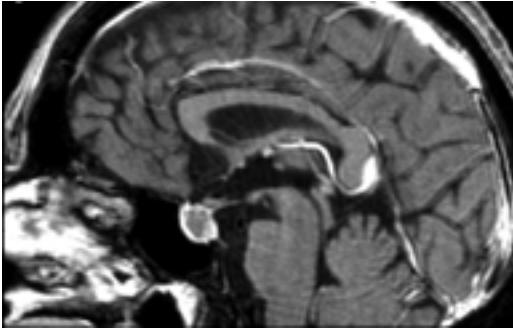


Fig. 1.39 Macroprolactinoma. Sagittal postcontrast T1GE image demonstrates a hypointense pituitary macroadenoma of ovoid shape

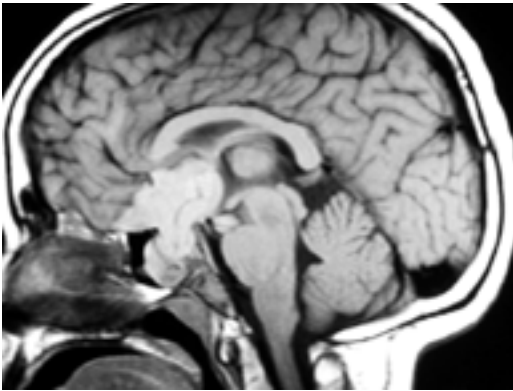


Fig. 1.40 Sagittal MR T1W image shows a large sellar and suprasellar mass also involving the sphenoid sinus in a young man with blindness. Planum sphenoidale meningioma

Nonfunctioning adenomas

Nonfunctioning pituitary adenomas are slow growing but invasive tumors occurring mainly in older adult patients. The tumors frequently extend into parasellar and suprasellar regions, cisterns, sphenoid sinus, cavernous sinus, and nasopharynx. Most of the nonfunctioning adenomas are diagnosed secondary to their complications – especially with visual disturbances and neurological symptoms. Large macroadenomas are nonhomogenous tumors with areas of necrosis and/or bleeding. Small nonfunctioning adenomas almost always represent incidental pathologic findings and belong to the group of

incidentalomas at the time of diagnosis. Clinical and biochemical examination of any incidentaloma is advised (see Chapter 1.4).

Note: According to our own experience the nonfunctioning pituitary adenomas are usually **macroadenomas** over 25 mm in diameter (75% of patients) in the time of diagnosis.

Nonfunctioning adenomas involve cavernous sinus, expand supra sellar, compress optic nerves and sometimes also foramina Monroe and the third ventricle. Patients are referred for imaging because of visual disturbances or with neurological symptoms (Fig. 1.41). Nonfunctioning adenomas are rare in childhood. The average age of our patients with nonfunctioning adenomas was 49.7 years. The nonfunctioning adenomas don't secrete hormones, therefore they are also called zero cell adenomas or 0-cell-oma.

Functioning adenomas

Functioning adenomas are named according to the particular hormone produced; such as prolactinoma (PRL-oma), growth hormone adenoma (GH-oma or STH-oma), adrenocorticotropin hormone producing adenoma (ACTH-

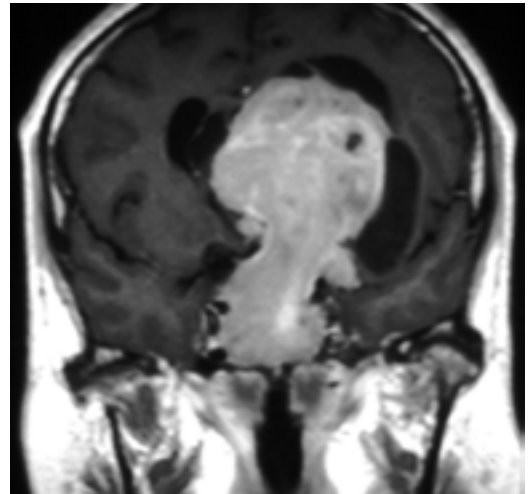


Fig. 1.41 Bitemporal hemianopsia. Coronal postcontrast Gd-DTPA T1SE scan shows a large nonhomogenous tumor involving the sella, sphenoid sinus, parasellar spaces and expanding high into the lateral ventricles

-oma), thyroid-stimulating hormone adenoma (TSH-oma), follicle-stimulating hormone adenoma (FSH-oma), or luteinizing hormone adenoma (LH-oma). The most common pituitary gland adenoma is prolactinoma which accounts for approximately 50% of hormonally active adenomas. The next most prevalent hormonally active adenomas of all secreting pituitary tumors are growth hormone producing adenomas (10%) and adrenocorticotropin hormone producing adenomas (10%). Thyrotropin secreting hormone adenomas are rare and represent less than 1% of pituitary tumors. The gonadotropins (FSH/LH) producing adenomas are also rare. These tumors usually occur in older patients. They are difficult to diagnose because of physiological hormonal changes in elderly people and especially in women in postmenopausal period. In younger persons they have been associated with hypogonadism or ovarian failure. Adenohypophyseal hormone producing cells have a very definite topographic representation within the gland. Prolactin secreting cells (lactotrophs or also called mammotrophs) and growth hormone secreting cells (somatotrophs) are located predominantly laterally. ACTH secreting cells (corticotrophs), TSH secreting cells (thyrotrophs) and FHS/LH secreting cells (gonadotrophs) tend to be located centrally. This is a finding of some clinical importance, as the location of adenomas parallels this distribution. Approximately 10% of active pituitary adenomas are plurihormonal, usually from lactosomatotrophs (prolactin and GH secreting tumors).

1.4.1 Hyperprolactinemia and prolactinoma

Prolactin is a hormone of adenohypophysis, produced in lactotroph cells, and its main role is to induce and maintain lactation in puerperium. Prolactin synthesis and secretion is suppressed by hypothalamic dopamine and dopaminergic agonists, and induced by estrogen, thyrotropin-releasing hormone (TRH), epidermal growth factor, oxytocin and dopamine receptor (D2) antagonists.

The clinical features of hyperprolactinemia may be divided into **hormonal** and in the case of macroprolactinoma the **local signs** (mass effect) may be present.

Hyperprolactinemia signs:

- Hypogonadism
- Infertility
- Galactorrhea
- Gynecomastia (in men)
- Mild hirsutism and acne (in women)
- Osteoporosis, osteopenia
- Hypopituitarism (larger macroprolactinomas).

Hypogonadism is caused by hyperprolactinemia-mediated sex steroid attenuation. High prolactin levels suppress by negative feed-back the production of gonadotropin-releasing hormone (GnRH) in the hypothalamus.

The local symptoms and signs:

- Headache
- Visual disturbances
- Bitemporal hemianopsia
- Hypothalamic disturbances (very large macroprolactinomas)

The headache is caused by the expansion of macroprolactinoma towards the diaphragma sellae and by its extension. The antral expansion of the tumor towards chiasma opticum may lead to bitemporal hemianopsia. Unilateral oppression of the optic nerve causes optic field disturbances, papilloedema and eventually optic nerve atrophy.

Hyperprolactinemia may have numerous etiologies besides prolactinoma, i.e. severe primary hypothyroidism, renal failure, pharmacological suppression of dopaminergic inhibition of prolactin secretion with various antidepressant and antipsychotic drugs or by pathological interruption or compression of the stalk (Fig. 1.42–1.47). The causes which can elevate prolactin level are summarized in table (Tab. 1.1). The most common cause of hyperprolactinemia is pituitary lactotroph adenoma – prolactinoma.

The clinical diagnosis of hyperprolactinemia is confirmed with the measurement of serum prolactin level and the serum sample should be obtained without excessive venopuncture

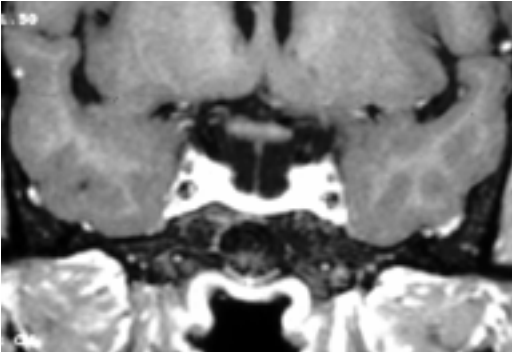


Fig. 1.42 Hyperprolactinemia. Coronal postcontrast T1GE image shows extension of cerebrospinal fluid into the sella turcica, the pituitary stalk extends to the floor of the sella (empty sella)

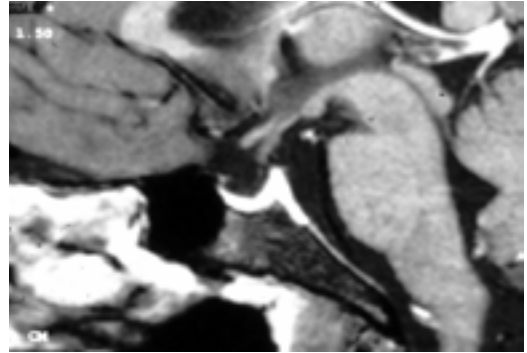


Fig. 1.43 Hyperprolactinemia. Sagittal postcontrast T1GE image shows extension of cerebrospinal fluid into the sella turcica, the rim of pituitary tissue is displaced posteriorly and inferiorly and the stalk is shifted dorsally (pituitary cyst? partly empty sella?)

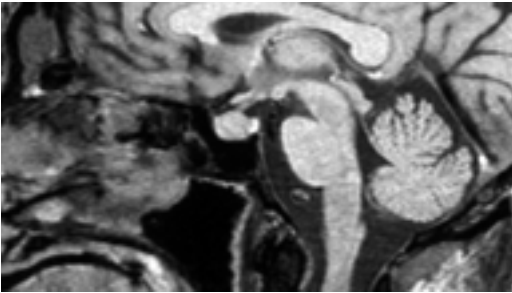


Fig. 1.44 Hyperprolactinemia. Sagittal plain T1GE image shows a superiorly enlarged adenohypophysis due to compression of the pituitary gland by ICA from both sides (pituitary pseudohyperplasia)

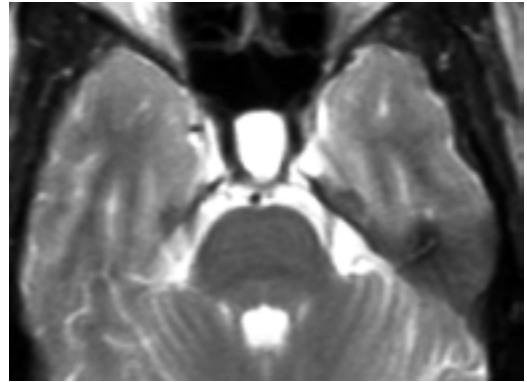


Fig. 1.45 Intrasellar cyst. Axial plain T2SE image shows a large cystic lesion in the sella region in the patient with hyperprolactinemia

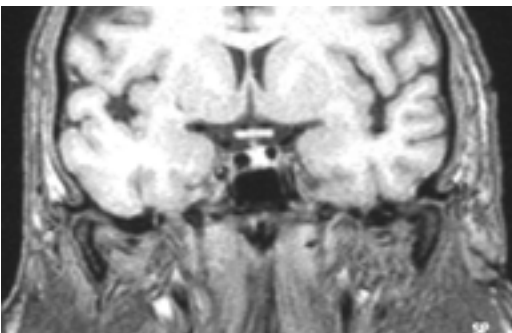


Fig. 1.46 Hyperprolactinemia. Coronal plain T1GE image shows pituitary gland compression by ICA from both sides

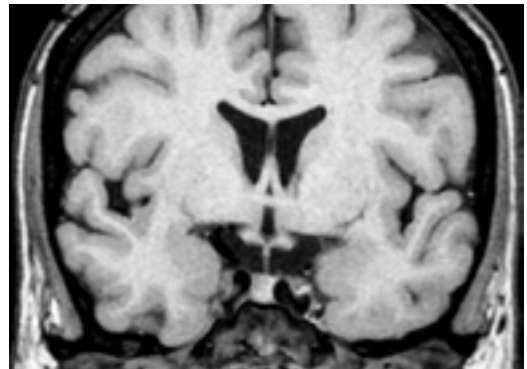


Fig. 1.47 Pituitary gland compressed by tortuous internal carotid arteries in a 33 years old female with hyperprolactinemia

Table 1.1 Causes of hyperprolactinemia

Physiologic	Pregnancy, breast-feeding, exercise, stimulation of nipples, stress
Pharmacologic	Antidepressant and antipsychotic drugs (e.g. phenothiazines, risperidone), some antihypertensive medication (reserpin, alpha-methyl dopa, Ca ²⁺ -channel blockers), opiates, cocaine, metoclopramide, estrogens
Pituitary	Micro- and macroprolactinoma, pituitary stalk compression or stalk section with nonprolactin secreting pituitary tumor or with parasellar mass, trauma
Hypothalamus	Infiltrative or degenerative changes – craniopharyngioma, meningioma, glioma, lymphoma, metastatic malignancy, tuberculosis, sarcoidosis, irradiation
Various	Renal insufficiency, primary hypothyroidism, acromegaly (co-secretion with GH), epileptic paroxysm, liver cirrhosis (rare), PCOS (mild elevation), herpes zoster (chest manifestation)
Neurogenic	Chest and spinal cord injury (stimulation of afferent nerve pathways)

stress. Dynamic testing for prolactin secretion is not necessary and is not further recommended. High levels of prolactin in patients without clinical symptoms and signs of hyperprolactinemia should be assessed for macroprolactin. This less bio-active form of prolactin (big prolactin and polymeric big-big prolactin) can easily be detected by the polyethylene glycol precipitation method. According to our experience the most frequent cause of hyperprolactinemia in patients referred to Endocrine clinic at the University Hospital in Bloemfontein was prolactinoma – Table 1.2 (Brunova et al., 2003).

Table 1.2 Causes of hyperprolactinemia (N 76)

Causes	Number	Percent
Prolactinoma	49	64.5
Idiopathic	11	14.5
Medication	6	7.9
Nonfunctioning adenoma	4	5.3
Craniopharyngioma	2	2.6
Empty sella	2	2.6
Hypothyroidism	2	2.6

Prolactinoma

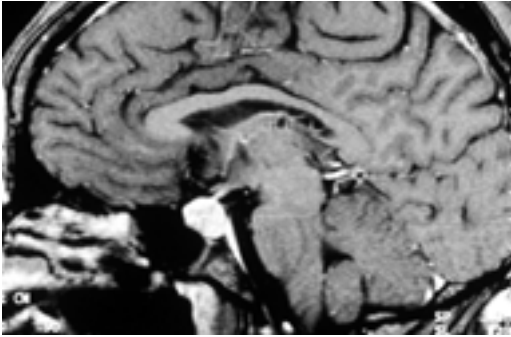
Prolactinoma is fairly the most common secreting adenoma, representing about 50% of secreting adenomas and about 40% of all pituitary tumors. The prolactinoma affects mainly

females from 15 to 45 years of age, with the mean prevalence approximately 10 per 100,000 in men and 30 per 100,000 in women. Patients of both genders with prolactinoma present with gonadal hypofunction, galactorrhea and in advanced cases with visual disturbances and headache. The clinical symptoms in females include infertility, amenorrhea, galactorrhea, headache, and visual problems; in males they include impotence, decreased libido, visual disturbances, and headache.

Reference values:

- Prolactin serum level:
F 44–880 pmol/l or 1–20 µg/l
M 89–720 pmol/l or 2–16 µg/l
(1 µg/l = 21.2 mIU/l)
- Recent reference values of our laboratory:
F 70–566 mIU/l
M 56–277 mIU/l
- 40% day-to-day variation in women, 10% in men
- The lowest in early afternoon, 2–3 times higher at night

The prolactin serum level in the blood is usually several times higher than the normal level (the normal level is under 20 µg/l). More than 70% of patients with prolactinoma have serum prolactin levels above 150 µg/l. A prolactin level greater than 250 µg/l usually indicates the presence of prolactinoma and a value of 500 µg/l suggests macroprolactinoma. On the other hand,



1.48 Hyperprolactinemia. Sagittal postcontrast T1GE image shows a stalk compression with prolactinoma

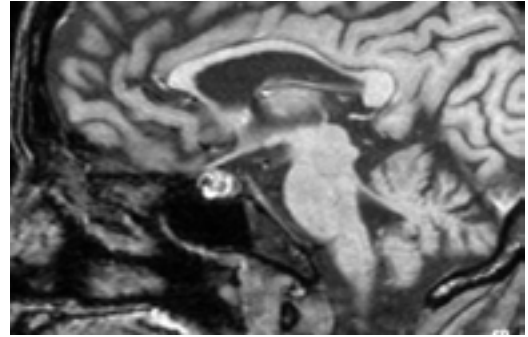


Fig. 1.49 Hyperprolactinemia. Sagittal postcontrast T1GE image demonstrates nonhomogenous intrasellar expansion with two hypointense lesions – two microadenomas of pituitary

the prolactin level does not always closely correlate with the size of the adenoma. Any mass compressing the pituitary stalk or hypothalamus diminishes the tonic inhibitory effect of hypothalamic dopaminergic factor and results in hyperprolactinemia (Fig. 1.48). Since different drugs and other circumstances can also produce hyperprolactinemia, it is important to exclude these causes before imaging investigation is begun. Except for prolactinoma and some selected drugs, none of these causes produce elevation of serum prolactin above 200 $\mu\text{g/l}$ and very rarely is prolactin elevated above 80 $\mu\text{g/l}$ from another reason than prolactinoma. However, sometimes a discrepancy between a very large macroadenoma and mildly elevated prolactin level is found. In that case it is necessary to eliminate falsely low prolactin levels (hook effect) with the serial dilution of serum samples.

Imaging. Hyperprolactinemia is the most frequent indication for pituitary imaging. There are no special imaging characteristics for a proper type of adenoma except that prolactinoma as well as somatotrophic adenoma are usually localized in the adenohypophysis eccentrically – mainly anteriorly-inferiorly or laterally – and not centrally.

After treatment with dopamine agonists, a decrease in size of the lesion, reduced permeability and shortened washout time in all types of pituitary prolactinomas have been described.

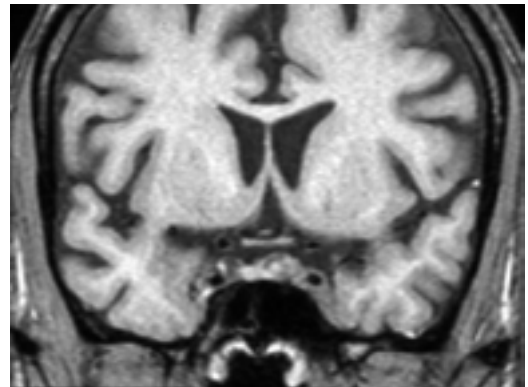


Fig. 1.50 Hyperprolactinemia – microprolactinoma with bleeding. Coronal plain T1GE image demonstrates nonhomogenous enlargement of the left part of the adenohypophysis with a round hypointense expansion and a hyperintense spot inside the mass

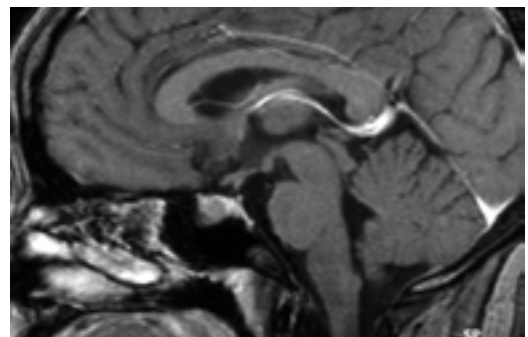


Fig. 1.51 Prolactinoma – hyperprolactinemia over 4000 IU. Sagittal postcontrast MR T1GE scan shows bilobulated hypointense expansion of the adenohypophysis with propagation into the sphenoid sinus

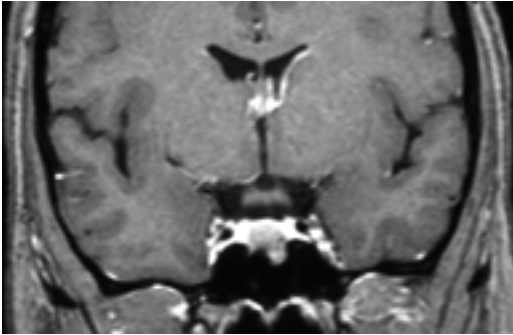


Fig. 1.52 Prolactinoma with tuberos expansion into the sphenoid sinus. Coronal postcontrast T1GE image demonstrates a marked lower intensity pituitary tumor in comparison with the signal intensity of the residual adenohypophysis

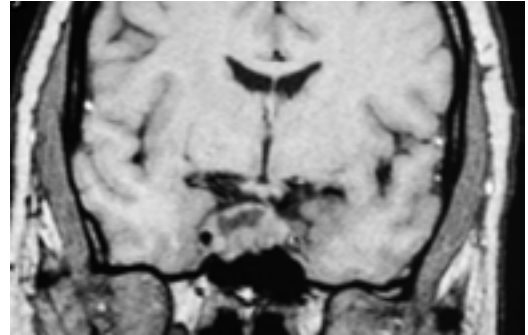


Fig. 1.53 Coronal MR T1 image shows nonhomogenous expansion of the right part of adenohypophysis

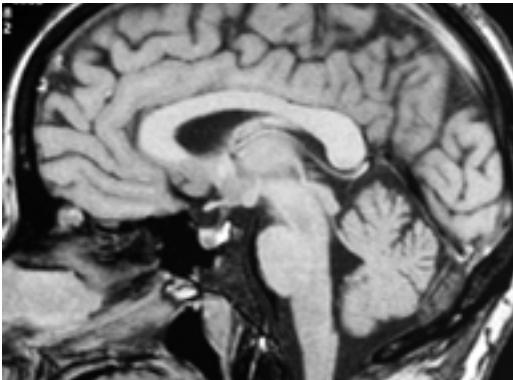


Fig. 1.54 Hyperprolactinemia. Sagittal MR T1W image shows a small round hypointense lesion of the adenohypophysis in a female 30 years old

Note: According to our experience the prolactinomas affect mainly females at the age of about 35 years. At the time of diagnosis 83% of prolactinomas were microadenomas under 10 mm in diameter. The shape of the tumor was round (48%) or oval (33%), less frequently lobulated (17%). Prolactinomas usually express a homogenous structure (in our study 73%), or infrequently cystic (11%), occasionally with bleeding into the adenoma (6%) (Fig. 1.49–1.54). Extraocular cranial nerves or cavernous sinuses were involved in large macroadenomas in most cases (Bruna, Brunova, 2003).

Treatment

The **main targets** of therapy:

- Suppression of high prolactin levels
- Control of tumor size
- Preservation, or improvement of the residual pituitary function
- Preventing the recurrence or the progression of hyperprolactinemia

Medical treatment. At first secondary causes of hyperprolactinemia such as hypothyroidism should be ruled out and treated if possible. In symptomatic patients, mainly with microprolactinomas, treatment with dopaminergic agonists (DA) is indicated. Among DA, bromocriptine and cabergoline are the first choice because of their efficacy. Treatment with bromocriptine (starting dose 0.625–1.25 mg p.o. in the evening has to be gradually increased to usual dose of 2.5 mg three times a day). Recently cabergoline is preferred because of its better tolerability (starting dose 0.25 mg per week, with usual dose 0.25 mg–3 mg/week, mostly 0.5 mg 1–2 times per week). Resistant prolactinomas require higher doses up to 11 mg per week.

Adverse effects of medical therapy may include mainly gastrointestinal disturbances and dizziness. Cabergolin use was related to the cardiac valve disease in patients with Parkinson's disease but this finding was not confirmed in patients treated with low dose of cabergoline.